

**Synthesis and Characterization of  
Graphene Nano-Composites (Graphene  
Oxide+ CoFe<sub>2</sub>O<sub>4</sub>) for Biomedical  
Applications.**



Khazima Muazim

NUST201362356MSCME67913F

**This thesis is submitted as a partial fulfillment of the requirements  
for the degree of**

**MS in (Nanosciences and Engineering)**

**Supervisor Name: Dr. Zakir Hussain**

**School of Chemical and Materials Engineering (SCME)**

**National University of Sciences and Technology (NUST), H-12**

**Islamabad, Pakistan**

**June, 2016**

## **Certificate**

This is to certify that work in this thesis has been carried out by **Ms. Khazima Muazim** and completed under my supervision in Surface Engineering Laboratory, School Of Chemical And Materials Engineering, National University of Sciences and Technology, H-12, Islamabad, Pakistan.

Supervisor \_\_\_\_\_

**Prof. Dr. Zakir Hussain**

Materials Engineering Department

National University of Sciences & Technology,  
Islamabad.

Submitted through

\_\_\_\_\_

**Prof. Dr. Mohammad Mujahid**

Principal/Dean,

School of Chemical & Materials Engineering

National University of Sciences and Technology, Islamabad

## **Dedication**

*Dedicated to my mother for her unwavering love and optimism, my father for being my foremost trusted advisor and my sisters for their being non-judgmental support system.*

## **Acknowledgement**

At First I am sincerely thankful to continuous supervision and guidance of my esteemed mentor Prof. Dr. Zakir Hussain Associate professor, (SCME, NUST). I would like to thank Dr. I.H Gul and Dr. Ahmed Nawaz for their constructive help towards the conducted research. I wish to thank principal SCME Prof. Dr. M. Mujahid and Faculty of SCME for providing congenial environment for research and study. I am thankful to Dr. Imran Hashmi (IESE) and Dr. Nasar-um-Minallah (ASAB) for facilitating my work at IESE and ASAB respectively.

I am greatly indebted to my friends Zehra Javed Malik, Sundas Khalid, Syeda Qudsia, Halima Tariq Bhatti, Ayesha Tabriz, Misbah Nazir and Bakhtawar Ghafoor for their care and concern. It was their friendship and belief in me that kept me steadfast and sane throughout this project

Nothing of this would have been possible without love, care, compassion, and strength of my family. From the core of my heart I would like to express my deepest gratitude to my Parents, my father for engraining in me the importance of hard work and self-confidence. My mother for her immense love and standing with me in all the thick and thins. My beyond “awesome” siblings for their patience, support and above all for their love. Special thanks are due to my brothers M.Tayyab and M.Tahir for making me laugh and for being a genuinely strong moral support.

**KHAZIMA MUAZIM**

## **Abstract**

Inorganic enzyme mimetics is a burgeoning area of research in field of nanoscience and materials engineering. These artificial inorganic enzyme mimetics provide leverage such as unparalleled flexibility and control over their design chemistry. In addition to this use of these artificial inorganic enzyme mimetics overcome hurdles for instance degradation of natural enzyme activity over a range of temperature, pH and solvents. These inorganic enzyme mimetics also provide improved limit of detection (LoD) with cost effectiveness.

In the research work carried out, two types of graphene oxide based cobalt ferrites nanocomposites were synthesized. In order to characterize and to elucidate their peroxidase potential techniques such as XRD, FTIR, SEM, AFM, UV Visible spectroscopy were used. These characterization techniques helped in revealing structural, morphological and chemical nature of designed composites. After this H<sub>2</sub>O<sub>2</sub> was used as peroxide analyte in order to detect the presence and extent of peroxidase like activity of the designed nanocomposites. Effect of dispersion of CoFe on GO sheets, effect of changing pH, temperature and concentration of GO-CoFe nanocomposites was elucidated.

Peroxidase like activity was found in both, physical and covalent composites however physical nanocomposite had LoD as 0.3 $\mu$ M in contrast to covalent nanocomposite which had LoD as 0.5 $\mu$ M. Physical GO-CoFe nanocomposite had better dispersion of CoFe particles on GO sheets . Whereas covalent nanocomposite was stable over wide range of pH and temperature.

It is anticipated that these enzyme mimetic GO-CoFe nanocomposites can be used as a signal transducer to develop a colorimetric assay for cancer cell detection and could be a powerful tool for wide range of applications in the field of biotechnology and biosensing.

## Table of Contents

Certificate.....	i
Dedication .....	iii
Acknowledgement .....	iv
Abstract .....	v
Contents .....	vi
List of Figures .....	viii
List of Tables .....	x
List of Abbreviations .....	xi
Chapter 1.....	1
1.1 Introduction .....	1
1.2 Problem statement.....	3
1.3 Objective .....	4
Chapter 2.....	5
Literature review .....	5
2.1 Introduction .....	5
2.2. Graphene oxide .....	6
2.2.1. Synthesis of Graphene oxide and its derivatives .....	6
2.3. Modification of GO.....	7
2.3.1 Covalent modification .....	8
2.3.2 Non-covalent modification .....	8
2.4 Magnetic nanoparticles .....	9
2.4.1 Synthesis of magnetic nanoparticles.....	10
2.4.2 Functionalization and stabilization of magnetic nanoparticles.....	12
2.4.3 Biocompatibility of magnetic nanoparticle .....	13
2.4.4 Physiology and fate of magnetic nanoparticles .....	13
2.5 Graphene Oxide Composites.....	14
2.6 Graphene oxide composites for theranostics (therapeutics and diagnostics).....	16
2.6.1 Drug delivery applications of graphene oxide composites (Therapeutics) .	16
2.6.2 Bio-sensing applications of graphene oxide composites (Diagnostics) .....	22
2.6.3 Introduction to biomimetic approach for peroxidase like activity towards Bio-sensing .....	26

2.6.3.1 Graphene- $Fe_xO_y$ magnetic nanocomposites as peroxidase mimetics catalysts .....	29
2.6.3.2 Tunable factors in peroxidase like activity .....	31
Materials and Methods .....	34
3.1 Synthesis of Graphene oxide (GO) .....	34
3.2 Synthesis of Magnetic nanoparticles/Cobalt ferrites ( $CoFe_2O_4/CoFe$ ) .....	35
3.3. Synthesis of oleylamine grafted GO .....	35
3.4 Synthesis of physical graphene oxide nanocomposite (GO-CoFe) .....	36
3.5 Synthesis of APTMS coated CoFe .....	36
3.6 Covalent synthesis of GO-CoFe nanocomposite .....	36
3.7 Analysis and characterization techniques used .....	37
3.7.1 X-Ray diffraction analysis(XRD) .....	37
3.7.2 Fourier Transform Infrared Spectroscopy (FTIR) .....	38
3.7.3 Atomic Force microscopy (AFM) .....	38
3.7.4 Ultraviolet Visible Spectroscopy (UV Vis) .....	39
3.7.5 Testing for Peroxidase like activity ( $H_2O_2$ detection) .....	39
Chapter 4 .....	40
Results and Discussion .....	40
4.1 Characterization of physical GO-CoFe nanocomposite .....	40
4.2 Detection of Peroxidase like activity of physical GO-CoFe nanocomposite .....	45
Mechanism of peroxidase like activity of GO-CoFe nanocomposite .....	48
4.3 Characterization of covalent GO-CoFe nanocomposite .....	50
4.4 Detection of peroxidase activity of covalent GO-CoFe nanocomposite .....	55
Chapter 5 .....	59
Conclusions and Future recommendations .....	59
References .....	62

## List of Figures

Figure 2.1 Enlisting various paths adopted for the nanoparticle clearance. ....	14
Figure 2.2 Depiction of modifications that can be made to modify GO.....	15
Figure 2.3 Tabulated illustration of applications of graphene oxide magnetic nanocomposites.....	15
Figure 2.4 Schematic illustration of synthesis of the FGOs and the dispersion of (a) GO and (b) the FGOs in an aqueous acetic acid solution ( $\text{CH}_3\text{COOH}/\text{H}_2\text{O}$ 0.2/1) copyright WILEY-VCH Verlag GmbH & Co. KGaA, Weinheim.....	18
Figure 2.5 Illustration of the remote opening of GO–polymer composite capsules using NIR-laserlight copyright The Royal Society of Chemistry.....	19
Figure 2.6 Photographs for the formation of the gel matrix based on 6 mg/mL GO nanosheets and 2mg/mL DOX copyright Elsevier Ltd.....	20
Figure 2.7 Schematic description of the GO–SNP sensing mechanism based on complementarity of nucleotide sequences given. Copyright The Royal Society of Chemistry.....	23
Figure 2.8 Schematic Representation of Colorimetric Direction of Cancer Cells by Using Folic Acid Functionalized PtNPs/GO. Copyright American Chemical Society.....	30
Figure 3.1 Tabulated illustration of experimentation, characterization and testing followed. ....	34
Figure 3.2 digital photograph showing washing of GO solution.....	35
Figure 3.3 Schematic illustration of APTMS coating on bare CF.....	36
Figure 4.1 Schematic illustration of formation of physical GO-CoFe nanocomposites.....	41
Figure 4.2 XRD pattern of (a) GO (b) Oleic acid coated CoFe and (c) physical GO-CoFe nanocomposite.....	42
Figure 4.3 UV vis spectra of (a) GO (b) physical GO-CoFe nanocomposite.....	43
Figure 4.4 SEM micrograph of GO (a) CoFe (b) physical GO-CoFe (c, d)nanocomposite with varying amount of OAM. ....	44
Figure 4.5 FTIR spectra of GO, GO-g-OAM, CoFe and physical GO-CoFe nanocomposite. ....	45

Figure 4.6 UV Vis spectra of (a) comparison of peroxidase activity of GO, CoFe and GO-CoFe nanocomposite and (b) TMB, TMB+ H <sub>2</sub> O <sub>2</sub> and physical GO-CoFe nanocomposite .....	46
Figure 4.7 Relative activity of physical GO-CoFe at various pH (a) and temperature (b). .....	47
Figure 4.8 Dependence of peroxidase like activity on varying concentration of physical GO-CoFe composite (20-100µg/ml).....	48
Figure 4.9 Linear calibration plot for H <sub>2</sub> O <sub>2</sub> detection using physical GO-CoFe nanocomposite. ....	49
Figure 4.10 Dependence of peroxidase activity by varying CoFe NPs on GO sheets. ....	50
Figure 4.11 Schematic illustration of formation of covalent GO-CoFe nanocomposite via amide linkage.....	51
Figure 4.12 XRD spectra of a) GO b) CoFe c)CoFe-APTMS d) covalent GO-CoFe nanocomposites .....	52
Figure 4.13 UV Vis spectrum of a) GO and b) covalent GO-CoFe nanocomposites..	52
Figure 4.14 SEM micrographs of a) GO b) CoFe c)CoFe-APTMS and d) covalent GO-CoFe nanocomposites. ....	53
Figure 4.15 FTIR spectrum of GO, CoFe-APTMS and covalent GO-CoFe nanocomposites.....	54
Figure 4.16 AFM analysis of GO(a) and GO-CoFe (b) covalent nanocomposites. ...	54
Figure 4.17 UV Vis spectra of (a) comparison of peroxidase activity of GO, CoFe and covalent GO-CoFe nanocomposite and (b) TMB, TMB+ H <sub>2</sub> O <sub>2</sub> and covalent GO-CoFe nanocomposite.....	55
Figure 4.18 Relative activity of GO-CoFe covalent nanocomposite a) pH and b) Temperature .....	56
Figure 4.19 Effect of increase in concentration of GO-CoFe covalent nanocomposite (20-100µg/ml).....	56
Figure 4.20 Linear calibration plot for H <sub>2</sub> O <sub>2</sub> detection using covalent GO-CoFe nanocomposite .....	57
Figure 5.1 Schematic illustration of proposed cancer cell detection mechanism using physical/covalent GO-CoFe nanocomposite.....	60

## **List of Tables**

Table 2.1 Peroxidase like activity of Graphene nanomaterials .....	27
Table 2.2 Peroxidase like activity of Graphene- iron oxide magnetic nanocomposites.....	30
Table 2.3 Enlisted advantages and disadvantages of using graphene nanomaterial as peroxidase like mimetics.....	31
Table2. 4 Tabulated illustration on use of GO magnetic nanocomposites for photo thermal therapy.....	25
Table 4.1 Brief tabulated comparison of properties of physical and covalent GO-CoFe nanocomposite.....	57

## **List of Abbreviations**

Graphene oxide	GO
Tissue Engineering	T.E
Magnetic cationic liposomes	MCLs
Reticuloendothelial system uptake	RES
3-Aminopropyltriethoxysilane	APTES
Polyethylenimine	PEI
Horseradish Peroxidase	HRP
reduced graphene oxide	rGO
Graphene family nanomaterials	GFN
chemical vapor depositions	CVD
(1-ethyl-3-(3-(dimethylamino)propyl) carbodiimide	EDC
N-hydroxysuccinimide	NHS
N,N'-dicyclohexylcarbodiimide	DCC
Poly (L-lysine)	PLL
Poly (acrylic acid)	PAA
Poly ethylene glycol	PEG
Poly (sodium 4-styrenesulphonate)	PSS
Bovine serum albumin	BSA
Cholesteryl hyaluronic acid	CHA
Superparamagnetic nanoparticles	SPION
Ultra-small superparamagnetic nanoparticles	USPION
Polyvinyl alcohol	PVA
Human Colon Cancer Cell line	HCT
Doxorubicin	DOX
Folate receptors	FA
Ellagic acid	EA
Poly (allylamine hydrochloride)	PAH
Near Infrared Radiation	NIR
Multiple drug resistance	MDR
Poly pyrrole	PPy

*List of Abbreviations*

Human immunodeficiency virus	HIV
Nicotinamide adenine dinucleotide	NADH
Prostate Specific Antigen	PSA
2,2'-azino- <i>bis</i> -(3-ethylbenzothiozoline-6-sulfonic acid)	ABTS
3,3',5,5'-tetramethylbenzidine	TMB
<i>o</i> -phenylenediamine	OPD

# Chapter 1

## 1.1 Introduction

Many carbon based materials have been in use for a long time now. These materials include graphite, diamond, fullerenes and carbon nanotubes. A relatively new addition to this family is graphene. Graphene has been hailed as wonder material due to its omnipotent properties[1]. Graphene is a single sheet of an atom thickness having  $sp^2$  hybridization arranged in a honeycomb like lattice, forming a 2D structure. In this lattice like structure each carbon atom is attached to another carbon atom in the same plane via covalent carbon/carbon bond. While the interlayers are arranged through weak van der waals forces. These forces are responsible for softness of this material. Presence of aromatic structure, free  $\pi$ -  $\pi$  electrons and reactive sites on the periphery are the reasons for its diverse usage[2].

These graphene sheets exhibit remarkably unique properties such as physiochemical and electromagnetic modulations. Many of these properties have been exploited by the scientists/researchers in various fields. Variety of applications of graphene are ranging from nano-electronics, nano-composites and solar cells to biomedical imaging, sensing, tissue engineering and drug delivery[3, 4]. Graphene exists in many forms Graphene sheets, graphene oxide and reduced graphene oxide. In this project my focus will be on graphene oxide (GO). Few of the properties of GO which makes it a point of choice in field of biomedicine especially in “theranostics” are as following.

It is biocompatible and biodegradable[5].It has large surface area ( $2630m^2/g$  approximately) and high aspect ratio for modification/s[6].It has un matched thermal conductivity i.e  $5000 W/m/K$ [7] It maintains a tendency to disperse well in aqueous medium (GO; hydrophilic derivative of graphene)[8]. It also has better colloidal stability compared to other carbon based materials). Graphene exhibits capability of traversing the plasma membrane[9]. It is believed to be cost effective and readily scalable[10, 12].

There are few existing challenges to the successful commercial application of graphene oxide. These challenges include

- Reproducibility of the functionalized graphene layers[11].
- Limited data available on *in vivo* and *in vitro* toxicity of graphene as biomaterial[2,13].

There are two kinds of modifications that are generally carried out to functionalize graphene nano-sheets, Covalent and non-covalent modifications. These non-covalent modifications include electrostatic, hydrophobic, Physi-sorption, hydrogen bonding and  $\pi$ - $\pi$  stacking. Presence of various functional groups such as epoxide, hydroxide and carboxyl groups provide endless possibilities to tailor covalent linkages to make desired system[14]. Both these modification techniques have been employed with variations and both have their own downsides. For example non covalent interactions are weak therefore show instability to external environment *in vitro* and *in vivo* while covalent modifications allow less quantity of drugs (aromatic) to be uploaded as GO sheets are also occupied by the coated polymers or other functional moieties[15].

Few of the intrinsic factors that affect the biomedical properties of graphene are as following.

Its morphology, thickness and degree of oxidation[16]. Besides graphene another family of nanomaterials that has been in limelight is one dimensional magnetic nanoparticles. Most explored magnetic nanoparticles are iron based, cobalt, manganese and zinc based ferrites. These ferrites are of special interest in the field of drug delivery, bio-imaging and magnetism driven applications such as hyperthermia[17].

Another important application that magnetic nanoparticles have garnered include magnetofection, magnetic immunoassay and magnetic force driven tissue engineering. Magnetofection methods are generally referred to delivery of nucleic acid vectors to the targeted cells where nucleic acid vectors are attached to magnetic nanoparticles. This magnetofection method provides several advantages over traditional transfection methods. These advantages include reduced process time (10 minutes in opposite to 2-4 hours), higher transfection rates with less vector dose and better efficacy[18]. Magnetic nanoparticles are used in immunoassays to detect the presence of various viruses and bacteria. Tissue Engineering (T.E) is another promising area of biomedical application. Magnetic nanoparticles has been employed in field of tissue engineering, cells are labelled with magnetic nanoparticles, these nanoparticles help cells to align under the influence of magnetic force[19]. This novel approach of magnetic tissue engineering was first proposed by Ito *et al*[20]. Magnetic cationic liposomes (MCLs)

were used to label keratinocytes. Their study showed that magnetically labelled keratinocytes were accumulated using external magnet while stratification was promoted to develop a sheet like 3D construct. In addition to their cellular effectiveness keratinocytes had accumulated 70% of total added MCLs[21]. The process of magnetic separation is not only limited to separation of analytes in biological sciences e.g. separation of genomic DNA but also to the separation of environmental pollutants such as mercury, arsenic and lead. The advantages of magnetic separation over separation techniques include the following. Less tedious; as pretreatment of active material is not a pre-requisite even for complex media, fast and highly versatile, cost effectivity, sorbent can be used after magnetic separation.

Like graphene oxide nanoparticles have large surface area, this surface area can be tuned by appropriate surface modification. This surface modification enable long circulation time and accumulation in lesions. These surface modifications provide stealth effect thus protecting them in biological environments and preventing non-specific binding and reticuloendothelial system uptake (RES)[22]. Many polymers and chemical moieties are used for surface modifications. Few of these surface modifying entities are as following Dopamine, Dextran, Chitosan, Alginate, Polyethylene Glycol, 3-Aminopropyltriethoxysilane (APTES), Polyethylenimine (PEI), Polyacrylic acid and Citrate[23, 24].

The effect of these stealth surface coating is imparted due to the functional groups that they bring along themselves e.g.  $-NH_2$  from oleylamine,  $-COOH$  and  $-COO$  from oleic acid, sodium oleate and Poly-acrylic acid and  $-OH$  from polyols, acetyl acetate anions. Other compounds which are used in coating are polymers e.g., dextran, sucrose and biomolecular peptides.

## 1.2 Problem statement

Though research and commercialization of graphene oxide and magnetic nanoparticle is underway for a long time now but the hindrance in complete successful biomedical application of graphene oxide [25] based magnetic composite is due to following reasons.

- Controlling size and homo-disperse population of magnetic nanoparticles on graphene oxide sheets.

- Detailed understanding about effect of surface functionalization on magnetic properties of nanoparticles and subsequently to graphene oxide composite.
- Physicochemical properties are changed once ferities/GO are functionalized[26]

### 1.3 Objective

The objective of the undertaken study is to make a graphene oxide based magnetic nanocomposite to lend its use towards biomedical sensing. In this study use of graphene oxide cobalt composite (GO-CoFe) will be assessed for its use in peroxidase like activity thereby leading to the detection of hydrogen peroxide ( $H_2O_2$ ). This composite will act as an inorganic enzyme mimetic nanomaterial catalyst leading to the detection of  $H_2O_2$ . Use of this inorganic nanomaterial as biomimetic enzyme has several advantages over the natural enzymes. They are stable over wide range of temperature unlike most of natural enzymes e.g. Horseradish Peroxidase (HRP) and can be used in presence of different solvents. These inorganic enzyme mimetics possess qualities such as ease of preparation at low cost, tunable catalytic activities and flexibility in structure design and composition. Properties such as ease of processing and storage add to their significant economic value. This peroxidase like activity is also demonstrated to be a distinguishing force to detect the abnormal cell formation thereby favoring the theranostic use of GO-CoFe nanocomposite. This GO-CoFe nanocomposite is more stable than natural peroxidase enzyme

# Chapter 2

## Literature review

### 2.1 Introduction

Graphene is a two dimensional layered  $sp^2$  hybridized material with worthy electrical, mechanical and thermal properties. In 2004 ground breaking discovery of an effective process through which a single layer graphene was made by Geim and colleagues[27]. This discovery led to the exponential research subsequently, the application of thinnest known materials in various fields. These fields largely were electronics, optoelectronics, photoconductive surfaces and biomedical imaging drug delivery and tissue engineering[28]. Graphene like graphite has each of its carbon atom attached to another carbon atom through strong covalent interaction however in contrast to diamond it has weak interlayer van der waals forces which makes it a soft material. It has carbon- carbon bonding in the plane while the presence of aromatic structure, free electrons and surface chemical moieties contributes to its exceptional electronic, optical and biomedical usage. This graphene material has been molded into various forms such as graphene oxide (GO), reduced graphene oxide (rGO) and graphene based composites. Thus a term was coined known as graphene family nanomaterials (GFN)[3].

In addition to this graphene based nanomaterial has lent its usage to the fabrication of functionalized bio-systems incorporating nucleic acid, peptides. Proteins and even cells. According to recent documentary aired by British Broad Casting (BBC) “Graphene: Technologies, Applications and Markets” Graphene based businesses are expected to project 67 \$ million worth by 2015 and 680 \$ million by 2020 with compound annual growth rate (CGR) of 58.7% in coming 5 years.

Numerous methods has been designed to extract graphene on laboratory scale. The primary and most well-known method is “Scotch- tape method”. This method leads to the isolation of defect free graphene sheets. Various other methods used are as following exfoliation based methods, chemical vapor depositions (CVD) [28], Pyrolysis, arc discharge, epitaxial methods, electrical assisted methods and chemical synthesis methods.

## 2.2. Graphene oxide

Graphene oxide (GO) is one of the analogues/derivative of graphite flakes. It is a highly oxidized form of chemically altered graphene. This Graphene oxide consists of single atom thick graphene sheet with carboxylic acid, epoxide and hydroxyl groups in a plane. Presence of carboxylate charges on the periphery provides negative charge to its surface and contribute towards its stability. In addition to this Epoxide and hydroxyl groups are present at the basal planes of it. These groups allow weak interactions and other surface reactions. The basal plane also happens to contain unmodified free  $\pi$  electrons which are hydrophobic in nature[29]. These  $\pi$  electrons enable the attachment of hydrophobic moieties to the graphene oxide sheet. Therefore it is rational to conclude that graphene oxide has amphiphilic sheet like character. Graphene oxide has properties which makes it a nanomaterial of choice. These properties are as following low cost, easily accessible and its ability to be scalable[30]. Ubiquitous use of GO has led to a novel class of materials termed as “Graphene Oxide based materials (GOBM)”[31]. As explained earlier Graphene oxide can be used in many fields i.e. electrochemical sensing, energetics, biological application and materials applications [32-34]. Among all these use of graphene has been made predominantly in the field biomedical engineering and energy materials[35].

### 2.2.1. Synthesis of Graphene oxide and its derivatives

Graphene oxide as explained earlier is a derivative of graphite flakes. Graphite flakes are polycrystalline particles which can be collected from natural sources or by synthetic means. Among these natural resource graphite flakes are preferred as they have localized defects in its aromatic structure which facilitate as seeding point for various chemical reaction processes. Two approaches are generally adopted for the synthesis of GO and its derivatives[36]. These two approaches are top down approach which aims at cleaving the multiple layers of graphite into single layers using mechanical, chemical and physical exfoliation methods. This top down approach is most commonly used[37]. Chemical exfoliation preparation of GO in general is carried by either Brodie, Staudenmaier or Hummers method. All the methods relies on oxidation of graphite flakes as starting step. Brodie and Staudenmaier uses potassium chlorate ( $\text{KClO}_3$ ) with nitric acid ( $\text{HNO}_3$ ) as an oxidizing agents. On the other hand side Hummers method avails the use of Potassium permanganate ( $\text{KMnO}_4$ ) and sulfuric acid ( $\text{H}_2\text{SO}_4$ ) as oxidizing agents. With the use of strong acid such as  $\text{HNO}_3$  and  $\text{H}_2\text{SO}_4$  graphite flakes

leads to the formation of graphite salts which act as precursors for subsequent oxidation of GO[38]. Hummer's method is the most abundantly used method of GO preparation now. Hummers method leads to the completion for GO preparation reaction within 2 hours and under 45 degree temperature. Hummer's method has been modified to accommodate use of more environment friendly reagents as hummers process itself leads to liberation of toxic gases such as NO<sub>2</sub> and ClO<sub>2</sub>. These modification of Hummers method includes [39]method designed by Kovtyukhova *et al* and Improved Hummers method established by Marcano et al[40]. Modified Hummers method utilizes H<sub>2</sub>SO<sub>4</sub>, KMnO<sub>4</sub> and NaNO<sub>3</sub> as oxidizing agent. Improved Hummers method has H<sub>2</sub>SO<sub>4</sub>, KMnO<sub>4</sub> and H<sub>3</sub>PO<sub>4</sub> as oxidizing agent. This improved hummers method yield large amount of hydrophilic GO and avoids releasing toxic gases[40]. Exfoliation process is excavated to include gentle approaches that lead to green, low waste and low cost production of GO material[28].

In addition to this, the second approach adopted for the preparation of GO includes bottom up approach such as Chemical Vapor deposition (CVD) where single layer of GO is deposited onto the selected substrate[41].

### **2.3. Modification of GO**

Modification of surface of GO leads to vital changes in the properties of GO that plays a crucial role in the biomedical application of GO. For instance addition of PEG not only improves the biocompatibility and solubility of GO but also it reduces the potential toxicity[22]. Its due to the surface modification of GO that enables magnetic nanoparticles, Gold nanoparticles and quantum dots to tethered to the GO or rGO sheets. Modification of GO surface helps conjugate various biologically useful and active entities to the GO sheets. These entities include well selected targeting ligands. Thereby GO sheet based system show specific and enhanced accumulation in targeted site[42].

In general surface modification of GO can be attained using either covalent or non-covalent modification. Covalent modifications often destroy some of conjugating entities of GO resulting in some properties being compromised. Whereas non-covalent modifications include methodologies such as  $\pi$ - $\pi$  stacking, electrostatic, hydrophobic

interaction and van der waals forces. Non covalent interactions help GO preserve the natural properties and structure[42].

### 2.3.1 Covalent modification

Covalent modification of GO is possible due to the presence of defects and reactive oxygen species in graphene's crystal lattice that serves as reactive site for covalent conjugations. Nucleophilic substitution, electrophilic addition, condensation and additions are various reaction through which covalent modification of GO is achieved. The main reactive site for the nucleophilic substitution are epoxy groups. Nucleophilic reaction between epoxy groups of GO and amino functional groups takes place when lone pairs of amino group attack epoxy group. Most advantageous aspect of these type of reactions are that they can be carried out in aqueous environment and at room temperature therefore becomes most promising method for large scale modification of GO[43-45]. Broad range of amine terminated molecules such as all kinds of aliphatic and aromatic amines, amine terminated small biomolecules, silanes, enzymes and nanoparticles. In order to carry out the covalent modification of GO materials various catalysts are used[46]. These catalysts utilizes well established chemistry of (1-ethyl-3-(3-(dimethylamino)propyl) carbodiimide (EDC) and N-hydroxysuccinimide (NHS) and N,N'-dicyclohexylcarbodiimide (DCC) for amide and esterification based bonding[47, 48]. Various polymers which are added to GO structure through amide and ester based modifications are as following poly (L-lysine) (PLL), poly (acrylic acid) (PLA), dextran, chitosan, aminosilanes and Poly ethylene glycol (PEG)[21, 47].

### 2.3.2 Non-covalent modification

Non covalent modifications encompasses interactions such as hydrogen bonding, coordinate bond, electrostatic interaction and  $\pi$ - $\pi$  interactions. Non covalent remains a popular approach for the modification of  $sp^2$  carbon materials such as CNTs and graphene. Non covalent functionalization of graphene material involves adsorption of polymer, surfactant, and small molecules/biomolecules such as DNA, porphyrins or peptides. Non-covalent interaction help yield many biomedical applications for GO based systems[49]. Stankovich *et al* was the first one to report non covalent interaction of graphitic nanoplatelets using poly (sodium 4-styrenesulphonate) (PSS). This non covalent interaction has been used to achieve theranostic use of GO platform. For example PEG grafted with poly (maleic anhydride-alt-1-octadecene) ( $C_{18}$ PMH-PEG)

was used to modify surface of rGO through strong hydrophobic interaction between hydrophobic graphene surface and long hydrophobic chains of C<sub>18</sub>PMH-PEG polymer. This modification has led to dramatically enhanced solubility of C<sub>18</sub>PMH-PEG-rGO at physiological conditions in addition to prolonging the half-life circulation of C<sub>18</sub>PMH-PEG-rGO[50].

Few of other surface modifying entities through non-covalent functionalization includes bovine serum albumin (BSA), polyoxyethylene sorbitan laurate (Tween), Pluronic F127, polyethylenimine (PEI) and cholesteryl hyaluronic acid (CHA). PEI was non-covalently attached to GO and this PEI conjugated GO was used for gene transfection. PEI conjugated GO had higher stability and less toxicity.

Many magnetic nanoparticles such as Fe<sub>3</sub>O<sub>4</sub>, TiO<sub>2</sub>, Pt, Pd, Cu, and Co<sub>3</sub>O<sub>4</sub> has been non-covalently tethered to GO sheets. These hybrid material were found to be useful towards drug delivery and photothermal therapy [51-59].

Few of these theranostic applications achieved through non-covalent interaction are discussed below[60].

## 2.4 Magnetic nanoparticles

Magnetic nanoparticles are one of the most vibrant and exploited nanomaterial. These nanoparticles finds their major application in various applications. These applications include their use in waste removal (heavy metals Pb and As), energy production (solar cells) and biomedical applications (MRI, drug delivery and biosensing and magnetic separation)[61]. A recent trend in magnetic nanoparticles reports the extensive research work on nano-zero valent Iron, core-shell nanoparticles and the less frequently used manganese, cobalt and Zn<sub>x</sub>Mn<sub>1-x</sub>Fe<sub>2</sub>O<sub>4</sub>ferrites. While iron oxides especially Magnetite (Fe<sub>3</sub>O<sub>4</sub>) and Maghemite (γ-Fe<sub>2</sub>O<sub>3</sub>) are widely studied and exploited in biomedical applications[62]. Due to their ease of preparation, chemical stability and the biocompatibility. These magnetic nanoparticles can be divided into 2 types based upon their sizes. Superparamagnetic nanoparticles (SPION) and ultra-small superparamagnetic nanoparticles (USPION). SPIONs are >50 nm in size while USPIONs are <50 nm in size. Most of the research surrounding this field of science elucidates and evaluates following of its aspects[63].

Synthesis methods and approaches, characterization analyses, effect and approaches for functionalization, effect of functionalization on their physiochemical properties, effect of their use in various composites and their applications[64].

Some of the terms used particularly for the description of magnetic nanoparticle containing nano-systems need to be precisely described for the future convenience. Few of these terms are as following.

**Solubilization verses dissolution:** as per IUPAC definition solubilization involves a short term micelle state formation. Solubilization system consists of a solvent, a colloid and the solubilizate whereas dissolution is a process where a solute completely forms a solution in the solvent. This solution is in form of colloidal dispersion rather than a true solution.

**Dispersion:** It is a process by which agglomerated nanoparticles are separated while a new interface is formed between solvent/ dispersion medium and the dispersed nanoparticles.

The phenomena of solubilization or dispersion is usually confused once CNTs or graphene materials are used with aqueous and non-aqueous solvents. This system can better be explained as dispersion phenomena[65].

The two key aspects of stability of the nanoparticles are as following.

**Kinetic stability:** this is the stability of the system in comparison to the gravitational forces. These comparative kinetics are also influenced by the Brownian motion, viscosity of the medium and the dispersion.

**Aggregation stability:** this stability determines the ability of the system to maintain its dispersity. This ability of the nanoparticles is particularly important towards the making of adsorption layer[66]. This adsorption layer is formed by the extracting low molecular weight ions from the solution.

#### **2.4.1 Synthesis of magnetic nanoparticles**

Numerous methods exist for the synthesis of nanoparticles. Few of these methods are as following. Co-precipitation method, micro emulsions, sol-gel syntheses, sonochemical reactions, hydrothermal reactions, thermolysis and electrospray methods[26, 67]. Synthesis of superparamagnetic nanoparticles is a difficult task due to their colloidal nature. Maintaining monodisperse population of magnetic grains of suitable size is major challenge. Whereas large scale reproducibility of adopted synthesis method is second most important concern. Synthesis method which do not require complex procedures such as ultracentrifugation, size exclusion chromatography and magnetic filtration are preferred for large scale synthesis. Preparing a homogenous population of ferrites within narrow range of distribution by using mentioned synthesis

method is difficult to follow. Few of most commonly used methods have been described in sufficient detail below.

### **Co-precipitation method**

Co-precipitation remains one of the most commonly used method for nanoparticle synthesis. Co-precipitation remains the most used, chemically easy and efficient pathway to follow for the synthesis of magnetic nanoparticles. Iron oxides are usually synthesized using stoichiometric mixture of ferrous and ferric salts in an aqueous environment. Size. Shape and chemical nature of nanoparticles is strongly dependent on various factors such as adjusting pH, ionic strength, temperature and nature of salts along the FeII/FeIII ratio[68, 69]. Particles size of nanoparticles ranging from 2-17 nm is obtained through this method. Factors such as acidity and ionic strength of the precipitation medium affects the particle size and size distribution of crystal structure, increased pH of medium leads to smaller particle size and wider size distribution of particles. Changes in pH affect the electrostatic surface charge of the particles.

Addition of organic anions such as carboxylates or hydroxyl ions or polymer complexing agents lead to controlled and homogenous sized nanoparticles as well. These carboxyl or hydroxyl providing agents include gluconic acid or oleic acid whereas polymers such as dextran, starch act as surface complexing agents.

Co-precipitation method proceeds in two stages. A short burst of nucleation occurs when concentration of involved species reach their critical supersaturation followed by slow growth of nuclei by diffusion of solutes to the surface of the crystal. In order to attain small size particles nucleation must be separated from grain growth phase.

The main advantage of co-precipitation method is large amount of nanoparticles can be synthesized using this method. However it is difficult to control the particle size distribution. The particle size distribution is difficult to control as only kinetic factors are the ones controlling the particle size distribution phenomena.

### **Hydrothermal or high temperature reaction**

High temperature reaction is carried out in aqueous medium in autoclave and reactors with temperature above 200° C and 2000 psi of pressure. Two main routes exist for the formation of ferrites in hydrothermal process. These two routes are called hydrolysis and oxidation or neutralization of mixed metal hydroxides. Ferrous salts are used in

former mentioned route. Reaction conditions such as solvent, temperature and time are few important factors having powerful impact on the properties of the product[70].

This method leads to highly monodispersed and size controlled particles. This happens due to the decomposition of iron organic precursors such as Fe(acetate) in the presence of surfactants or organic solvents such as octyl ether or oleic acid[71].

It was observed that the prolonged reaction time and higher water content leads to larger Fe<sub>3</sub>O<sub>4</sub> particles. In the hydrothermal method, a balance shared between nucleation and grain growth is the key to attain smaller size particles. Nucleation occurs faster at higher temperature leading to smaller size particles. Whereas prolonged reaction time favours the grain growth resulting in larger particle size.

Size and morphology of the nanoparticle is not only maintained using temperature and time constants but also by concentration, ratio of reactants, precursor, complexing strength and nature of solvent.

### **Sol-Gel method**

Synthesis of nanostructured metal oxide in wet route is attained by sol-gel method. This method is based on hydroxylation and condensation of molecular precursors in the solution. Thereby generating nanometric solution of particles[72]. Further condensation and polymerization of metal oxide framework leads to wet gel formation/ since both the sol-gel reactions occurs at room temperature further heat treatment is required for final crystallite state formation. The main parameters that influence the particle properties in sol-gel methods include solvent, temperature, nature, concentration of salt precursors employed, pH and agitation[73].

This sol-gel method provides advantages such as i) materials with predetermined structure can be obtained according to experimental conditions ii) considerable control of homogeneity and microstructure is provided iii) molecules such as silica can be embedded in the sol-gel matrix which maintains their stability and properties of the particles iv) there exists a possibility to obtain pure amorphous phases and monodispersed particles.

### **2.4.2 Functionalization and stabilization of magnetic nanoparticles**

Functionalization and stabilization of nanoparticles go hand in hand. Functionalization of nanoparticles is usually performed in order to increase the compatibility, solubility and to increase the conjugation sites. Functionalization can be carried out directly after the reduction step of the metal salts or by step by step substitution of the primary

polymer coating by another compound. Among most commonly used surfactants in the first step includes sodium oleate, oleic acid and oleylamine. Oleic acid is most commonly used to provide a dense protective layer thereby providing highly uniform and monodisperse particles. This oleic acid coated nanoparticle will be highly soluble in organic solvents such as toluene, hexane and chloroform. Dopamine remains another important surface functional group which not only provides stealth property to the aggregated particles but also helps to conjugate various biomolecules to it. Among all the functionalization processes the use of water soluble remains a key approach to yield water soluble magnetic material system. These water soluble polymers include polyethylene glycol (PEG), diethylene glycol (DEG), triethylene glycol (TREG) and polyvinyl alcohol (PVA)[74].

Stabilization of magnetic nanoparticles is crucial to obtain colloidal stability of the ferrofluids in the biological and magnetic media. The stability of the colloidal suspension is result of equilibrium attained using attractive and repulsive forces. Four kind of forces that contribute to the inter particle stability are as following. Van der Waals forces, electrostatic repulsive forces, dipolar forces and the steric forces. Controlling the strength of these forces is of key importance to obtain particles with good stability.

#### **2.4.3 Biocompatibility of magnetic nanoparticle**

Concerns have been raised regarding the safety issues of nanoparticles however recent studies have shown that the ferrites are biocompatible and has shown no hemolytic potential with negligible toxicity. Results of research conducted on adult mice confirms that the ferrites were biocompatible even once they were used beyond the safety dosage approved for human use. This certainly demonstrate their biotechnological and nano-medicinal usage.

The therapeutic and nano-medical properties of these systems are highly dependent upon their physicochemical properties such as permeability, stability, morphology (size, shape and functionality) and biocompatibility. Usually the biocompatibility of the material is determined by the type, orientation, and structure of the involved materials and the hybrid[75].

#### **2.4.4 Physiology and fate of magnetic nanoparticles**

Once magnetic nanoparticles are injected inside the human body i.e. affected desired area. These nanoparticles are subjected to diverse biological events. These particles are

coated by plasma proteins through a process known as opsonization. These opsonized particles are recognized by the body's defense mechanism Reticuloendothelial system (RES). RES is diffused system with specialized cells capable of eating up the inert/foreign material (phagocytosis)[76]. This system is extended to liver, bone marrow spleen and lymph. In order to circumvent this RES elimination the surface of nanoparticles has to be modified by their surface modification. This surface modification will make them biocompatible, non-toxic and stable towards RES. It has also been established that the hydrophobic nanoparticles are rapidly coated and cleared by the RES while in contrast to this hydrophilic nanoparticles are comparatively better resisted towards the RES. Therefore most magnetic nanoparticles employed for the biomedical usage are maintained to be hydrophilic in nature (Figure 2.1). In order do so these magnetic nanoparticles are coated with polymers such as Polyethylene glycol (PEG), Polyethylene Oxide (PEO), Dextran, Chitosan and Polyoxamines[77].

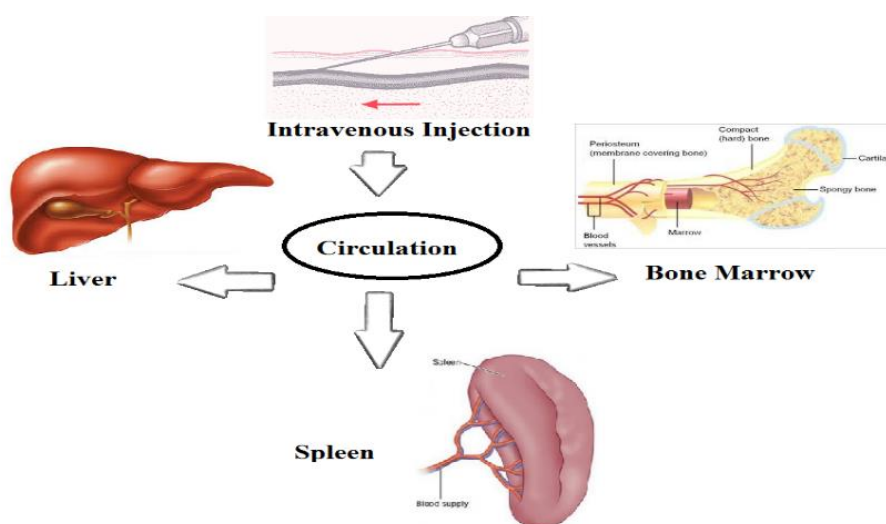


Figure 2.1 Enlisting various paths adopted for the nanoparticle clearance.

## 2.5 Graphene Oxide Composites

Reasons of remarkable properties of GO are mainly associated with the possibility of its chemical modifications as well as combine effects with various entities such as polymers and magnetic nanoparticles (Figure 2.2). Since GO tends to aggregate under the physiological conditions (due to the presence of salts, ions and proteins) thereby reducing the proposed effectiveness, its modifications not only retain its effectiveness but also reduce toxicity of the other component.[78-80].

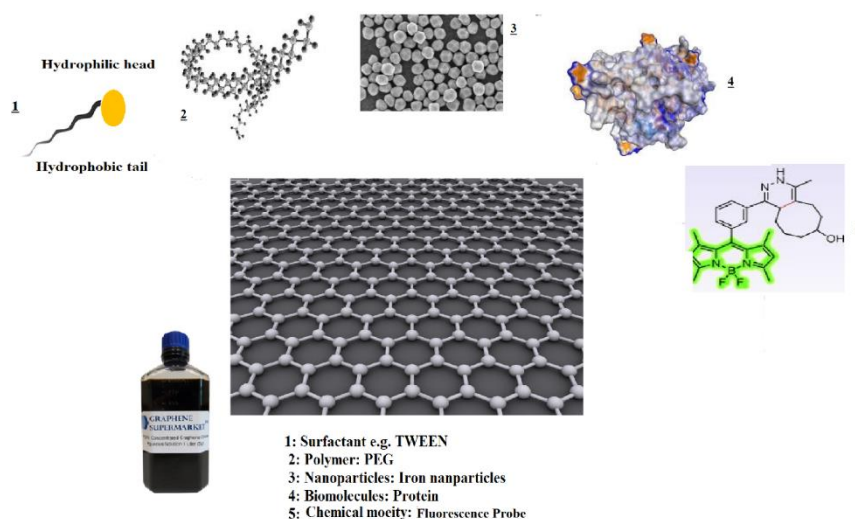


Figure 2.2 Depiction of modifications that can be made to modify GO.

Most of the composites include chemical moieties that provide biocompatibility (e.g. PEG, PVC) [81, 82], thermo/stimuli responsiveness (e.g. poly (*N*-isopropylacrylamide) (PNIPAM)[8, 15], enhance mechanical properties (PMMA, PVC) [6], used for the surface coating of the biomaterials (e.g. dextran, polyamide 11)[83]and enhance colloidal stability (Sulfonic acids, Oleylamine) [84].

Therefore, a lot of research for the use of graphene based composites highlights its use in drug delivery applications, magnetic resonance imaging, fluorescence imaging[85], antibacterial activity [86], biosensors[87, 88]) and hyperthermia [89, 90] (Figure 2.3).

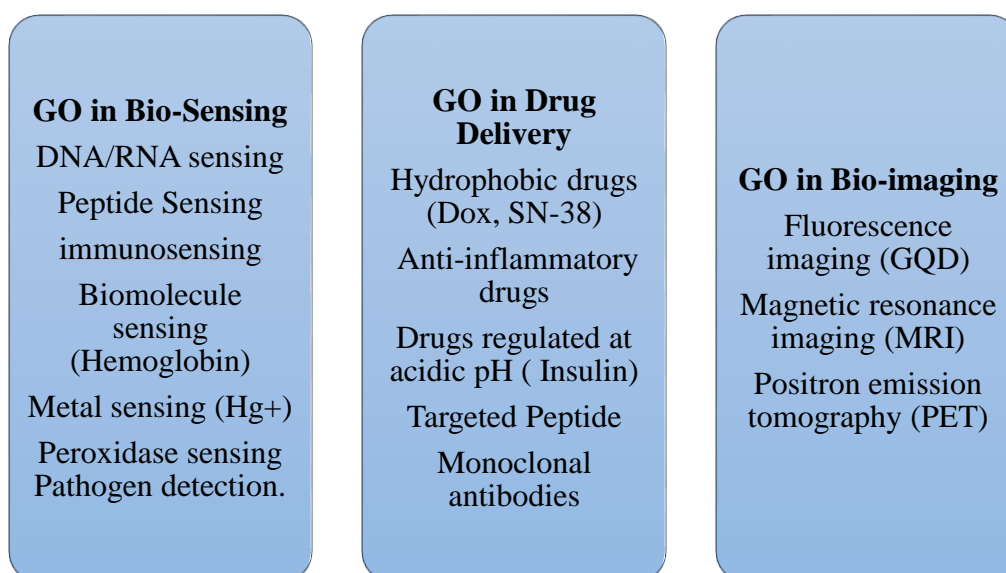


Figure 2.3 Tabulated illustration of applications of graphene oxide magnetic nanocomposites.

## 2.6 Graphene oxide composites for theranostics (therapeutics and diagnostics)

### 2.6.1 Drug delivery applications of graphene oxide composites (Therapeutics)

GO, due to large surface area, exposed functional groups and free  $\pi$  electrons, accommodate loading of less soluble drugs onto it without reducing the efficacy of drugs [91]. Maintaining the efficacy of therapeutic drugs is a major driving force behind drug delivery research. In order to maintain the efficacy of drugs, long term sustained release of drug through blood circulation is required. SN 38 is considered as water insoluble drug and its dispersion is an issue which hampers its potency to attack colon cancer cells. Dai *et al.*, used polyethylene glycol (PEG) conjugated graphene nanosheets with non-covalent adsorption of SN38. This non covalent adsorption was driven by hydrophobic interaction and  $\pi$ - $\pi$  stacking. Through this system they were able to attain slow controlled release along with high potency i.e. IC 50 value 6nM for Human Colon Cancer Cell line (HCT cells) in comparison to its pro-drug, a hydrophobic analogue Camptothecin (CPT-11). Further this group used PEG-NGO for the targeted delivery of Rituxan (CD 20 antibody) and Doxorubicin (DOX). This system exhibited pH dependent drug release [92].

Zhang and colleagues tested the ability of graphene nanosheets to carry multiple/mixed anticancer drugs at a time. This approach was one of its kind and also significant to reduce drug resistance occurring for many cancer treatments thereby reducing their efficacy over time. They had used NGO functionalized with sulfonic acid groups which was decorated later with folate (FA) receptors through covalent binding. Addition of folate receptors enable the direct uptake of drugs which were loaded to FA- NGO matrix. The loading capacity of Dox and CPT drugs was equal to their single loading. Although therapeutic efficacy was increased but cytotoxicity to Human breast cancer cell line (MCF-7) was reduced. Efficacy was increased due to its specificity to deliver drug only to cancer cells [93].

Following the pursued, Kakran *et al.*, functionalized GO with hydrophilic and biocompatible polymer such as Tween 80, Pluronic F38 and maltodextrin and the functionalized GO was further used as a nanocarrier for poorly water soluble anticancer drug, ellagic acid (EA). For the very first time EA was loaded onto functionalized GO using  $\pi$ - $\pi$  interaction. Release kinetics as well as cytotoxicity of the loaded drug formulation was evaluated at various pH. This functionalized GO carrying EA was

further tested to target MCF-7 and human colon Adenocarcinoma cells (HT29) [94]). It was established that GO did not hamper the antioxidant activity of loaded EA.

Exfoliated graphene oxide's chemical reduction is the most common approach adopted for the preparation of reduced graphene nanosheets (GNS). However, use of hydrazine as reagent contaminates nanosheet thus limiting its use in drug delivery. In a recent research Liu *et al.*, have investigated the use of green and facile synthesis method where gelatin was used as reducing reagent and also as functionalized moiety. It was concluded that Gelatin-GNS was biocompatible, non-toxic and soluble in aqueous medium and various physiological fluids (PBs, FBS and DMEM). This Gelatin-GNS was also tested for its drug carrying capability for DOX where drug was taken up by the cells in a sustained released manner through gelatin mediated endocytosis. The significance of this study was the use of facile and green synthesis method where possible risk of contamination was restricted [95]. Similar facile and cost effective routes have also been developed for the preparation of reduced GO[44].

Another research group led by Yang *et al* in 2011 has explored the drug carrying capacity of graphene sheets through dual target functionalization and pH sensitivity. In this research surface of GO sheet was functionalized with targeting ligand folate receptors (FA) and super paramagnetic iron oxide nanoparticles ( $\text{Fe}_3\text{O}_4$ ). Multiple functionalized GO was able to demonstrate the targeted and pH responsive drug delivery. In this setting GO was decorated with  $\text{Fe}_3\text{O}_4$  while 3-aminopropyl triethoxysilane (APS) was use to coat  $\text{Fe}_3\text{O}_4$ . This coating served as mediator to attach FA to GO- $\text{Fe}_3\text{O}_4$  composite [19].

It has also been investigated that hybrid graphene nano-sheets with chitosan (FGOCs) show improved solubility in aqueous acidic medium and such functionalized hybrid showed marked controlled drug release behaviour. The drugs tested in this hybrid system were Ibuprofen and 5 fluorouracil. Microscopic techniques such as SEM and AFM were used to scan the topographic features of the functionalized graphene sheets. It was the first report on the adsorption of aromatic moiety containing drugs tested on graphene sheets and concluded that FGOCs has better cellular penetration and hence has better chances of success in its use in drug delivery.

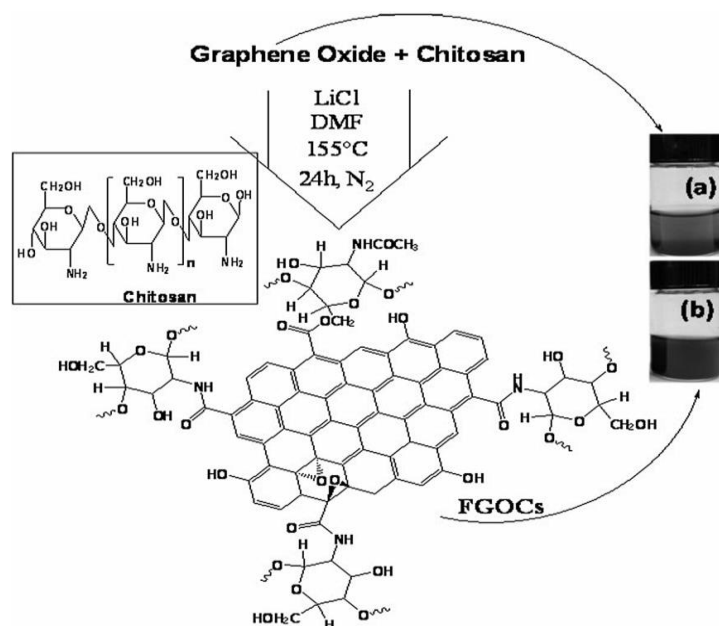


Figure 2.4 Schematic illustration of synthesis of the FGOCs and the dispersion of (a) GO and (b) the FGOCs in an aqueous acetic acid solution (CH<sub>3</sub>COOH/H<sub>2</sub>O 0.2/1) copyright WILEY-VCH Verlag GmbH & Co. KGaA, Weinheim.

Controlled release formulation has been made using biocompatible GO and the biodegradable chitosan. In this formulation GO was loaded with Dox while later on it was encapsulated with folate conjugated chitosan. This formulation had shown its immense potential as targeted and control delivery nanocarrier as this formulation was sensitive to acidic environment (Figure 2.4)

In another study GO was grafted via facile amidation reaction with chitosan (CS). This CS-g-GO was tested for its drug carrying whereas gene delivery potential was also tested. It was concluded that the CS-g-GO was able to carry CPT which resulted in higher toxicity towards HepG2 and HeLa cell lines than the pure drug. Similarly gene delivery potential was illustrated through the delivery of CS-g-Go with plasmid DNA in stable and complexed form into the HeLa cell lines[96]).

In another study, effect of AuNPs on drug delivery was investigated where AuNPs were either doped or grown *in-situ* on the GO sheets. This nanocomposite consisting of AuNP/GO showed efficient drug delivery in the Hela cell lines. Such nanocomposite can also be exploited towards intracellular Raman Imaging[97]

In 2012, Kurapati used GO along with LBL microcapsules (poly (allylamine hydrochloride) (PAH) where the composite was stimuli responsive towards near infrared light. The GO-PAH microcapsule released encapsulated drug Dox in a point wise fashion upon Near Infrared Radiation (NIR)-laser ablation. This laser ablation

generates local heating effect which in turns lead to the release of drug from microcapsule. In addition to excellent optical and permeable properties of GO, it has also enhanced the mechanical strength of the microcapsule thereby preventing its breakage during intracellular delivery[91]. Following images (Figure 2.5) give a clear illustration how microcapsule release drug in point wise fashion [98].

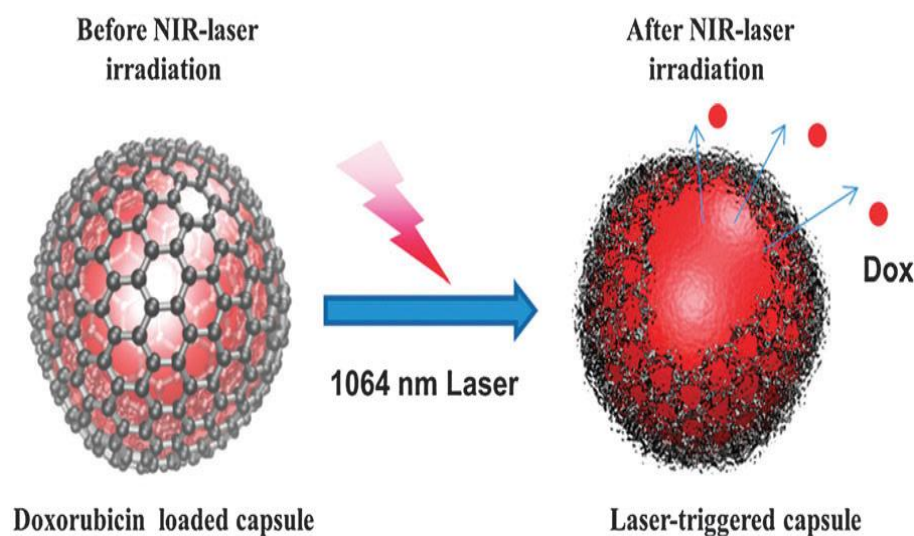


Figure 2.5 Illustration of the remote opening of GO–polymer composite capsules using NIR-laser light copyright The Royal Society of Chemistry.

GO has not only been used as stimuli responsive drug delivery system but also for gel based drug delivery system. Due to recent emphasis on the use of gel matrices for the delivery of drugs such as doxorubicin hydrochloride, CPT, 5-fluorouracil, paclitaxel, cisplatin and adriamycin, exploiting the strength of novel materials is of significant importance[18, 99]. In order to attain these gel formulations various polymers are generally used through physical and chemical cross linking where chemical cross linkers such as photo initiators are used. These species though contribute good mechanical strength but are deemed inappropriate toward biomedical applications. In a recent research, GO has been used to encapsulate doxorubicin hydrochloride through gel matrix. The crucial edge of this research was that none of the polymers or chemical matrix was used except GO which was used for *in situ* gelation effects (Figure 2.6). Doxorubicin was released in a sustained released manner. GO-Dox gel exhibited good mechanical strength and good inject ability [100]. Another aspect of the use of this GO based hydrogel is their capacity to self-heal, carry various biomolecules (DNA) or dyes [101].

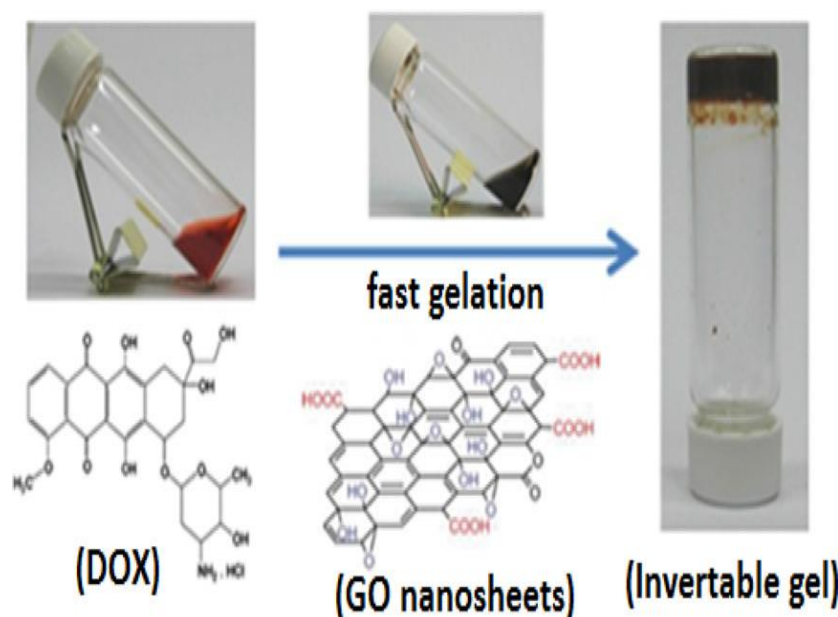


Figure 2.6 Photographs for the formation of the gel matrix based on 6 mg/mL GO nanosheets and 2mg/mL DOX copyright Elsevier Ltd.

In another remarkable work exploiting drug carrying capacity of GO, Yang et al., used the principle of multiple supramolecular assembly to create a GO scaffold for drug delivery[102]. In this approach three components were used 1) folic acid modified  $\beta$  cyclodextrin, a target unit 2) adamantanyl porphyrin as linker and 3) GO as carrier unit. It was observed that due to the presence of folic acid modified  $\beta$  cyclodextrin GO nanocarrier could recognize FA receptors on cancer cells thereby increasing the effectiveness of Dox in comparison to free Dox.

In an attempt carried out by Wu et al., it was demonstrated that the effects of drug resistance in breast cancer cells could be avoided using GO loaded with Adriamycin. Adriamycin was physically loaded onto the GO sheets and was pointed out that the GO-ADR caused effective reversal of ADR resistance in MCF/ADR cells with reversal index of 8.35. Similarly, in another study, dual usage of GO platform was exploited where [103] authors used the ability of GO to carry single stranded DNA/RNA with ease and its loading capacity towards the anti-cancer drugs through  $\pi$ - $\pi$  interaction was investigated[104].

Bcl-2 which is considered to be an important anti-apoptotic defence protein which leads to multiple drug resistance (MDR) [105]. This drug resistance can be avoided by knocking down the protein's expression where the role of siRNA is extremely important since knockdown of Bcl-2 expression will not only inhibit MDR but also

make cancer cells sensitive towards the anti-cancer drugs. Chemically grafted GO with polyethylenimine (PEI) was used as a nanocarrier to Dox and the Bcl-2 targeting siRNA. This study showed that the PEI-GO can effectively be used as a nano-carrier and for the sequential delivery of Bcl-2 targeted siRNA. This dual effect led to the significantly enhanced chemotherapeutic efficacy. In another study, GO coupled with PEG-FA was used to carry hTERT siRNA for the intracellular delivery of siRNA [106]. In this research GO was conjugated with PEG-FA in order to make it bio-compatible and selective. In addition to this siRNA was loaded onto the graphene sheets with the help of 1-pyrenemethylamine hydrochloride through  $\pi$ - $\pi$  stacking. This GO-PEG-FA-PyNH<sub>2</sub> carried hTERT siRNA led to significant silencing of mTRET expression in HeLa cell lines. This was confirmed through RT-PCR and the western blotting

In another study, hybrid of PEI modified GO with oleic acid was created which was further modified by up conversion nanoparticles (UCNP) and superparamagnetic nanoparticles. This hybrid (PEI-GO) was used as nano carrier of hydrophobic nanoparticles and resulted in the transferring of hydrophobic nanoparticles from organic phase to a water soluble phase. PEI-GO-UCNP hybrid exhibited 100% weight loading of Dox drug. This drug carrying hybrid showed higher killing potential towards cancer cells in *in vitro* environment drug carrying potential of this hybrid was complimented by the luminescence properties due to the UCNP [107].

In a recent study, Szunerits *et al.*, demonstrated that the composite of magnetic nanoparticles coated with 2-nitrodopamine and GO could be used for the effective delivery of insulin without damaging the native state of insulin in the acidic environment. Loading capacity of GO and GO composite was extremely high for insulin where  $100\pm 3\%$  was loaded on to GO sheet while  $88\pm 3\%$  was loaded on to GO-MP<sub>dox</sub> matrix. Insulin loaded onto GO-MP<sub>dox</sub> nanomatrix was protected from gastric secretions and acidic environment while drug was released once exposed to basic environment (pH= 9.2) [108]. The drug delivery potential and effectiveness of GO based composites can be increased using various preparation techniques[44, 109]. One of the studies which evaluated the difference in the efficiency of GO composites synthesized using *in situ* and ferro-fluid techniques. In this study it was exhibited that the GO carrying iron oxide nanoparticles in the form of ferrofluid demonstrated higher

toxicity towards the MCF-7 cell lines due to higher iron content, higher loading efficiency of the drug (Anastrozole) and smaller particle size[110]). Recently GO has also been conjugated with targeted peptide of chlorotoxin (CTX) through 1-ethyl-3-(3-dimethylaminopropyl) carbodiimide (EDC) and NHS. This CTX-GO was further loaded with Dox through non covalent interactions. This CTX-GO-DOX showed significant improvement towards the treatment of gliomas. Conjugated GO was not only able to deliver drug specifically to the glioma cells but has also proved to maintain sustained release [111].

In another recent study, GO was deposited inside a conducting polymer, poly pyrrole (PPy) scaffold to prepare nanocomposite which was demonstrated to show enhanced electrical properties. These electrical properties were further used for the release mechanism of dexamethasone which was loaded on a conducting nanocomposite [112].

### **2.6.2 Bio-sensing applications of graphene oxide composites (Diagnostics)**

GO has been exploited as an essential material for bio-sensing applications since the energy transfer electron donor/acceptor molecules are exposed at planar surface making GO an efficient candidate for long ranging quenching [113].

Some of the fascinating applications of graphene nanocomposites reported so far include its use in DNA sensing, protein sensing and protein assays. To explore the ability of GO as molecular probe *in situ* and *in vivo*, Wang and coworkers investigated graphene nanosheet and aptamer with carboxyfluorescein (FAM/GO-nS) where graphene nanosheet was used as sensing plate and aptamer as molecular probe[34]. Since aptamers have specificity and sensitivity for the target, the target in this case was a fungi toxin (Ochratoxin A) secreted by *Aspergillus ochraceus* and *Penicillium verrucosum*. In this case Adenosine triphosphate (ATP) aptamer was used which was non-covalently bonded to GO nanosheets. It was demonstrated that GO sheets have the ability to protect aptamer/DNA molecule from enzymatic cleavage activity and also leads to fluorescence quenching (Figure 2.7). Both these properties make it a strong contender for DNA/RNA/ protein cargo for gene delivery and for bio-labelling for cellular imaging respectively.

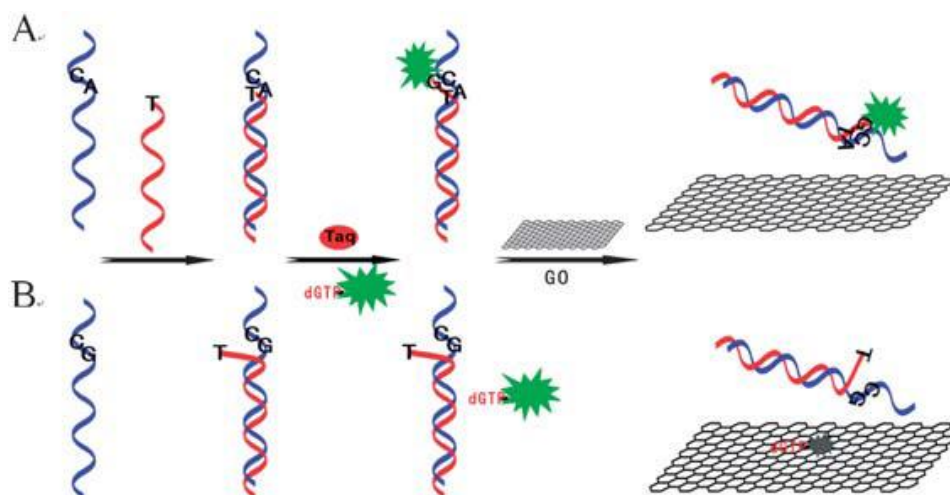


Figure 2.7 Schematic description of the GO–SNP sensing mechanism based on complementarity of nucleotide sequences given. Copyright The Royal Society of Chemistry.

Luo *et al.*, in 2012 reported a convenient and enhanced chemiluminescence (CL) biosensor for sequence specific DNA detection. It was previously known that GO has fluorescence quenching property and was presumed that it has CL property too. In this study Human immunodeficiency virus (HIV) oligonucleotide sequence associated with the HMDNAzyme (PHIV) was used as a model probe. In this mechanism, this probe (ssDNA) once mixed with GO was assumed to be adsorbed to the GO surface through  $\pi$ - $\pi$  interaction between ssDNA nucleoside/nucleotides and GO. Since HMDNAzyme stimulates CL in the presence of luminol and  $\text{H}_2\text{O}_2$  [114] and the probe ssDNA assumed to hybridize with the complementary target DNA, the presence of dsDNA assumed to be released from the GO causing significant increase in CL emission. This system was further suggested to have potential for sequence specific detection not only for DNA but for other biomolecules as well.

Similarly, another research group has reported the photoluminescent (PL) properties of graphene quantum dots (GQDs). These GQDs has shown excitation and solvent biased PL behaviour. Once GQDs were excited from 400 to 540 the PL peaks were shifted from 515 to 570nm but with a significant decreased intensity. Also PL peak shifted from 475 to 515nm for different solvents since GQDs were sensitive towards solvent being used. These GQDs were developed by single step solvothermal method. The PL quantum yield was as high as 11.4%. Such GQDs have advantages such as being biocompatible, low cytotoxicity and no photobleaching effect[115] and show great promise for future research.

Another example of using GO as peptide biosensing platform has been illustrated in another recent study [116]. In this approach it was proposed that GO-peptide complex can be used for real time, specific and time dependent detection of cancer biomarker. This study shows that since GO was already at quenching state due to the binding of RGD-Pyrene by  $\pi$  stacking to that of GO, the quenching state was restored by the competitive binding of RGD with Integrin  $\alpha\beta3$  where Integrin was found to play important role in the development of cancer cell's adhesion and proliferation.

GO based sensing has also enabled scientists to overcome many limitations such as distance in the designing of efficient and sensitive FRET based biosensors. One of the studies carried out lately [117] demonstrated the use of fluorescence accepting property of GO while CdTe quantum dots as F1 donor entity to pave a way for the hepatocellularcarcinoma immuno-sensor. In this system GO was conjugated with capture antibody 1(Ab1) while QDs were modified with reporter protein (Ab5) where AFP acted as a bridge. Ab1/AFP/Ab5 led to the development of self-assembled complex which resulted in the quenching of QD's emission. This GO based immuno sensor bridged the distance dependent limitations in the case of traditional immuno-sensors.

In addition to sensing of DNA, GO based composite has also been used for the detection of protein. In order to detect protein, protease substrate linker was attached between energy transfer donor quantum dots and the energy acceptor GO leading to a GO-quantum dot nanoprobe. In a similar attempt, extremely sensitive insulin detection was reported[118]. It was demonstrated that GO-aptamer binding events can compete with target aptamer binding events resulting in the release of aptamer from the GO surface leading to the sensing of insulin. Furthermore, it was demonstrated that this aptamer can further be amplified employing amplification technique using DNase I enzyme. This amplification strategy led to 100 fold higher sensitivity than the traditional 1:1 binding assays while LOD reported was 5nM

Another exciting area of graphene oxide used is in area of photothermic therapy. Some of the most recent work has been summarised in the table 2.4.

Table 2. 4 Tabulated illustration on use of GO magnetic nanocomposites for photothermal therapy.

Composite	Drug/molecule loaded	Highlight of the research	Reference
GO-Au@PLA		Gold nanoparticles were grown into the PLA microcapsules followed by GO layers encapsulation leading to effective photothermal ablation.	[119]
rGO-Cu <sub>2</sub> O Nanocrystals		rGO with Cu <sub>2</sub> O crystals used for specific visible and infrared light irradiation	[52]
rGO	Hypocrellin A and Camptothecin	HA/SN-38/GO leads to the combinatorial photodynamic and chemotherapy	[120]
GO-BaGdF <sub>5</sub> -PEG		Enhanced stability for passive targeted PTT	[121]
PEGylated-GO	NIR fluorescence dye Cy5COOH	Synergistic use for the photoacoustic imaging and PTT	[122]

Few studies show the functionalization of GO with polyoxyethylene sorbitol anhydride monolaurate (TWEEN-20) [45] where TWEEN-20 was reacted with GO through hydrogen bonds as well as through Van der Waals forces [123]. This TWEEN-20 functionalized GO was further grafted with AuNP through *in-situ* chemical reduction of gold salts. Such AuNP/TWEEN-20/GO nanocomposite showed good catalytic activity towards hydrazine oxidation and the reduction of 4-nitrophenol and demonstrated the promise of exploiting in bio-sensing as well as in the environmental monitoring. Similarly, in another study, GO was GO modified with hydroxypropyl- $\beta$ -cyclo-dextrin (HPCD) and tetra-phenyl-porphyrin(TPP) as an electron transfer

molecule which led to demonstrate excellent electro-catalytic activity by detecting haemoglobin reduction or oxidation at the detection limit of  $5 \times 10^{-9}$  M[124]. GO, magnetic nanocomposite is also used for photothermal therapy and cancer cell ablation

### **2.6.3 Introduction to biomimetic approach for peroxidase like activity towards Bio-sensing**

Natural enzymes, mostly proteins are linear chain of amino acids that can fold and self-assemble to yield a three dimensional structure. This three dimensional structure is the reason behind the specific activity of enzymes. Natural enzymes act as biocatalysts to large array of biological processes with high specificity and selectivity however under the mild conditions (pH, temperature and pressure). Constrains such as denaturation upon exposure to the harsh environment, high cost of purification, storage strict the wide technological applications of natural enzymes. This in consequence led to the pursuit of alternative molecules that can overcome said challenges. These molecules are man-made and artificial in nature.

Artificial enzymes a term coined by Ronald Breslow for enzyme mimics (Biomimetics; mimicking nature or biology) emerge as a promising and exciting subject. These artificial enzymes are highly efficient alternative materials that in general follows principles of natural enzymes. Over the years enzymes mimics have evolved from molecular to nanoscale resulting the formation of highly organized materials for biological activity. Nanomaterials are arranged in sophisticated hierarchical manner to generated Nano architecture which generated a significant impetus for mimicking the nature of nanofabrication techniques. A complex interplay between surface structure, morphology and physicochemical properties results in outstanding properties.

Peroxidases are a large family of isoenzymes found in all living organisms. Peroxidases are classified as mammalian or plant peroxidases ranging in molecular weight 35,000 to 100,000 Da. Peroxidases typically catalyse a biological reaction in which  $H_2O_2$  is reduced whereas substrate act as a redox electron donor. Few of the naturally occurring peroxidases are Nicotinamide adenine dinucleotide (NADH), phosphate peroxidase, horseradish peroxidase (HRP) and iodide peroxidase. HRP is a routinely and abundantly used peroxidase as chemical reagent in organic synthesis and in a clinical and bioanalytical chemistry.

Few of more applications of HRP includes the following.

- Dye decolourizations

- Degradation of lignocellulosic biomass for biofuel production.
- Bioremediation of waste water for the removal of phenolic and amine contamination[125]
- Detection of antigens and antibodies through ELISA[126].
- Delignification of wood pulp.

HRP follows a ping pong mechanism or non-sequential mechanism also known as double displacement reaction. In this mechanism enzyme tends to change from its intermediate state to its standard state. Another key feature of ping pong mechanism is that one substrate is converted into product and dissociates and releases before the second substrate binds. In order to detect peroxidase like activity of biomimetic enzymes formation of both oxidized product and consumption of  $H_2O_2$  are calculated[127].

The concentration of  $H_2O_2$  can be measured by attaching a color changing chromophores such as 2,2'-azino-*bis*-(3-ethylbenzothiozoline-6-sulfonic acid) (ABTS), 3,3',5,5'-tetramethylbenzidine (TMB), and *o*-phenylenediamine (OPD) which upon oxidation give green, blue and yellow color respectively. Rate of reaction is determined by monitoring absorbance intensity changes as function of time. At fixed concentration of catalyst several kinetic runs are performed by varying concentration of  $H_2O_2$  or the chromophore. The kinetic parameters such as reaction velocity ( $V_{max}$ ), Michaelis-Menten constant ( $K_m$ ) are determined by straight line plot such as Lineweaver-Burk plot[128]. Graphene along its derived nanomaterials has been utilized for peroxidase like activity following table summarises work that has been established in this regard so far table 2.5). Several functional nanoscale materials have shown their potential for peroxidase enzyme mimics. AuNP, cerium NP, magnetic NP, platinum NP, manganese dioxide NM, bimetallic nanostructures and carbon based NM are particularly notable. In this regard. Owing to their unique and efficient characteristics these enzyme mimics have been used for biosensing, environmental protection, immunoassay and theranostics. Graphene remains the most recent material to intersect its usage in enzyme mimetics.

Table 2.5 Peroxidase like activity of Graphene nanomaterials.

Nanomaterial	Method	Substrate	Application	Reference
Hemin-Graphene	colorimetric	TMB	SNP detection	[129]
DNA-Hemin-graphene	Colorimetric	TMB, OPD, ABTS	Hg <sup>+2</sup> and DNA detection	[130]
Hemin-Graphene	Electrochemical	Hydroquinone (HQ)	Micro RNA detection.	[120]
Graphene-AuNP	Colorimetric	TMB, ABTS and OPD	DNA detection	[131]
rGO-Au composite	Colorimetric	TMB	H <sub>2</sub> O <sub>2</sub> detection	[132]
GO-AuNP	Colorimetric	TMB	Hg <sup>+2</sup> and Pb <sup>+2</sup> detection	[133]
Au-rGO	Colorimetric	Pyrogallol	Dye removal	[134]
FA-GO-AuNC	Colorimetric	TMB	Cancer cell detection	[135]
Graphene quantum dots (GQD)	Colorimetric detection	TMB	Cholesterol detection	[136]
GQD + ZnFe <sub>2</sub> O <sub>3</sub>	Electrochemical detection	TMB	DNA detection	[137]
GQD+ Fe <sub>3</sub> O <sub>4</sub>	-	TMB	Removal of phenolic compounds	[131]
Pt NP + GO	Colorimetric	TMB, OPD and HQ	Cysteine detection	[138]

### 2.6.3.1 Graphene- $\text{Fe}_x\text{O}_y$ magnetic nanocomposites as peroxidase mimetics catalysts

Among all the graphene hybrid nanomaterials graphene-magnetic nanocomposites are a class of nanomaterials which have gained much popularity due to the properties of magnetic nanoparticles which are stable over wide range of temperature and pH.

In a study, it was established that COOH modified GO has an intrinsic peroxidase activity which can extend its use for glucose detection. In this report, catalytic property of GO was investigated through the use of peroxidase substrate (3,3,5,5-tetramethylbenzidine (TMB)). GO through its intrinsic peroxidase activity catalyzes the TMB substrate into blue color product. GO-COOH has high catalytic ability compare to the naturally occurring Horse reddish peroxidase (HRP) enzyme. This ability of GO-COOH has been exploited for highly selective glucose detection. The level of glucose detected was as low as  $1 \times 10^6 \text{ mol L}^{-1}$  while its linear range of the detection was  $1 \times 10^6 \text{ mol L}^{-1}$  to  $2 \times 10^5 \text{ mol L}^{-1}$ . It was demonstrated that this GO-COOH can be used for medical detection[139]. GO-COOH was found to be not only highly selective but also has advantages such as ease of preparation, low cost and stability. Based on the similar intrinsic peroxidase activity of the GO, it has been further exploited for the immunosensing towards Prostate Specific Antigen (PSA). In this approach magnetic beads were modified with anti-PSA antibody (Ab1) while GO was modified with Ab2 making the entities an immunocomplex, sandwiching antigen protein PSA. Once the reaction was complete, magnetic beads were removed while the concentration of Ab2-GO was calculated due to color change (Colorimetric), exhibiting as if it reacts with hydroquinone and  $\text{H}_2\text{O}_2$ . This study established the evidence that GO can be used for the selective and point of care tool for clinical diagnosis [140]. Similarly, in another study, it was reported that the intrinsic peroxidase like property of GO can be enhanced once it was decorated with iron ferrites ( $\text{Fe}_3\text{O}_4$ ) [141]. Kinetic parameters of the study supported that the catalytic activity was enhanced under the provided settings. Following table exhibits the improvement made in the peroxidase activity of the GO based ferrites composites (Figure 2.8).

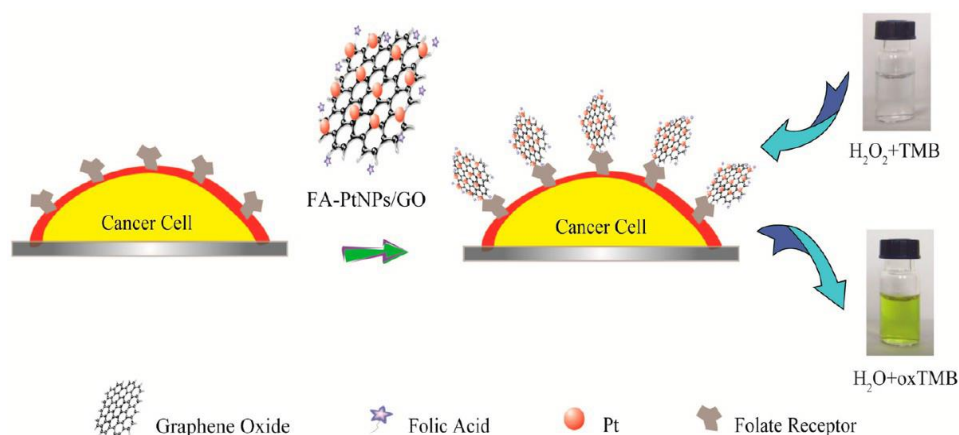


Figure 2.8 Schematic Representation of Colorimetric Detection of Cancer Cells by Using Folic Acid Functionalized PtNPs/GO Copyright American Chemical Society.

In a continuation, another study demonstrated the use of nanocomposite prepared from rGO and cobalt ferrites which exhibited higher reaction and subsequently higher catalytic (peroxidase) activity towards the substrate (TMB). This composite was prepared by the use of PVP as reducing agent and stabilizer and showed not only higher catalytic activity but also higher stability in the presence of different solvents and at various temperatures. However at optimum conditions, the detection limit of this nanocomposite was 0.3  $\mu$ M which was higher than many other ferrites based colorimetric sensors [133]. It has also been demonstrated in number of recent reports that both Iron [141, 142], platinum and cobalt [143] based composites with GO having the ability to mimic enzyme like activity are likely to play an important role in biotechnology [144] and environmental detection [145]. Recently Mn ferrites have also been explored for the colorimetric detections/ peroxidase activity [146]. However, such composites of GO with manganese ferrites for peroxidase activity are still to be explored.

Some of other graphene based magnetic composites for peroxidase like activity has been identified in the list table 2.6. 2.6.3.2 Tunable factors in peroxidase like activity

Peroxide like activity of graphene nanomaterial can be tuned further by modulating several factors such as pH, temperature, size of nanomaterial, fabrication of composite with controlling the ratio of individual components and use of modulators such as bio-receptors. Lee and park's have demonstrated how manipulating the wt% ratio of different metal nanoparticles on GO surface has led to higher catalytic activity. It was seen that GO-MNP- 10 (km 0.144) have greater affinity than the GO-MNP-30 (km

0.237). In another study effect of deposition of metal ions on the surface of nanohybrid systems was proved to increase the enzymatic activity of nanomaterial. In this study it was seen that the peroxidase like activity of AuNP-GO hybrid was decreased after binding to the antibodies. However activity of nanohybrid was enhanced once Hg+2 was added to nanohybrid.

Table.2.6 Peroxidase like activity of Graphene- iron oxide magnetic nanocomposites.

Nanomaterial	Method	Substrate	Application	Reference
GO-Fe <sub>3</sub> O <sub>4</sub>	Colorimetric	TMB	Glucose detection	[147]
rGO- Fe <sub>3</sub> O <sub>4</sub>	Colorimetric	TMB	Acetylcholine detection	[148]
GO-Pt-	Colorimetric	TMB	Cancer cell detection	[149]
GO-Hemin-MNP	Colorimetric	ABTS	Glutathione (GSH) detection	[150]
Au-Fe <sub>3</sub> O <sub>4</sub> -GO	Colorimetric	TMB	Hg+2 detection	[151]
Co <sub>3</sub> O <sub>4</sub> -rGO	Colorimetric	TMB	H <sub>2</sub> O <sub>2</sub> detection	[152]

Tunability of these nanomaterials is carried out by looking into the advantages and disadvantages of presented material. Some of these advantages and disadvantages are as following table 2.7.

Table 2.6 Enlisted advantages and disadvantages of using graphene nanomaterial as peroxidase like mimetics.

<b>Advantages</b>	<b>Disadvantages</b>
Large surface area and functional groups to allow bioconjugations.	Use of chemical reagents during synthesis and functionalization raises environmental and health concerns.
Size, shape, structure dependent tunable properties	Data on health safety is insufficient and not concrete.
Easy rational design, recycling, purification and recovery.	Limited use of substrates other than TMB.
Easy dispersion in aqueous medium.	Low efficiency, specificity and selectivity is reported in many cases.
Operational stability at harsh conditions	A lot effort is required for the diversified biosensing mechanism.

### 2.6.3.3 Challenges and future prospects

Despite exhibiting much potential, there still remains a large room for improvement that can be made by future research. Few of these challenges are enlisted as following.

- Graphene based materials are prominently being used for many cellular applications. However they are not devoid of hemolytical and cytotoxic effects. The surface physicochemical are largely responsible for the adverse effects. Therefore in light of this knowledge, efforts are to be under taken to translate promising scientific results into practical applications.
- Precious elements such as Pt and Pd are to be replaced by less expensive materials with comparable and higher catalytic efficiencies. In this regards magnetic nanoparticle based graphene composites and visible light driven peroxidase like activity materials are favored and likely to mature in future.
- Another area where peroxidase like activity is likely to play its role is detection of biologically important anions such as cyanide anions. These anions are known to cause acute toxicity to the living organisms.

- Factors such as attaching modulators influencing the catalytic activity of nanomaterials are important to explore to undergo the possible limitations even at high temperature and pH.
- Technical loopholes or misconceptions related to the nomenclature of graphene nanomaterials are important to tackle for scientific integrity.

In short, on demand sophisticated surface engineering of graphene based nanomaterials for peroxidase activity based bio-sensing is likely to thrive in near future.

# Chapter 3

## Materials and Methods

Experimentation work was carried out in three major steps. These three major steps are as following.

<b>Experimentation</b>	<b>Synthesis or formation of GO/ CF composites</b> oleylamine modified GO + CF with oleic acid = GO-CF (Physical composite) GO + amine terminated CF= GO-CF (chemical composite)
	<hr/> <b>Charaterization of Material</b> XRD FTIR SEM AFM UV Vis spectroscopy
	<hr/> <b>Application based testing</b> Peroxidase activity

Figure 3.1 Tabulated illustration of Experimentation, characterization and testing followed.

### 3. Experimentation and characterization

#### 3.1 Synthesis of Graphene oxide

Synthesis of graphene oxide was carried out using Improved Hummer's Method. Modified Hummer's method was chosen due to various reasons such as it is environmental and biological friendly in nature. It is cost effective and easy to carry out.

Following was the procedure adopted to synthesize graphene oxide.

Synthesis of GO was carried out using Improved Hummer's Method. Graphite flakes (3.0g) were mixed with KMnO<sub>4</sub> (18.0g) and mixture of H<sub>2</sub>SO<sub>4</sub>/H<sub>3</sub>PO<sub>4</sub> (9:1; 360:40ml) was stirred for 4-5 hours while temperature was maintained at 35-40° C. After this step

temperature was raised upto 50 ° C and maintained as such for 12 hours under stirring. The reaction was brought to room temperature, ice (400ml) and H<sub>2</sub>O<sub>2</sub> (5ml) was added to the quench the reaction. At this step the solution turned into mustard color. IM HCl was added into the solution to give it an acidic wash. Subsequently after this step, acid washed pellet was centrifuged at 4000rpm several times with water till the pellet of the solution had attained pH 7.



Figure 3.2 Digital photograph showing washing of GO solution.

### 3.2 Synthesis of Magnetic nanoparticles/Cobalt ferrites (CoFe<sub>2</sub>O<sub>4</sub>/CF)

Cobalt ferrites nanoparticles were synthesized using co-precipitation method. In first step 0.2M (100ml) of Iron nitrate and 0.1M (100ml) cobalt nitrate were mixed with ultrapure water. These aqueous solutions were stirred and heated up to 90° C. Ultrapure water was used to avoid impurities and particles aggregation. Upon reaching 90° C both Co and Fe solutions were mixed and heated to attain 90° C temperature. On the other handside NaOH (3M; 100ml) aqueous solution was prepared. Once NaOH aqueous solution attained temperature 90° C, both Co+ Fe and NaOH solutions were mixed. At this step specified amount of oleic acid (2.5ml) was added as surfactant to the solution. This mixed solution was maintained at 90° C for half an hour. After 30 minutes, heating was stopped while solution was brought to room temperature (RT) with continuous stirring. Solution at RT was washed twice with distilled water and ethanol at 3000rpm for 15 minutes. This washing lead to the removal of uncoated fatty acid. Precipitates obtained were dried overnight at 100°[153]. After the drying of precipitates the obtained powder was grinded to obtain finer particles. Overnight dried particles were annealed at 600° C for 8 hours.

### 3.3. Synthesis of oleylamine (OAM) grafted GO

GO flakes (40mg) were mixed with OAM (10ml) and chloroform (14ml). This mixture was sonicated for 30 minutes. After sonication solution was washed in order to remove the unreacted oleylamine, washing was performed by mixing equal volume of ethanol

into the solution. This solution was centrifuged at 4000rpm for 30 minutes (figure 3; step 1 (b)). The precipitates obtained were re-dispersed into chloroform again. In contrast to GO itself OAM modified GO had good dispersion in chloroform.

### 3.4 Synthesis of graphene oxide composite

Composite of CF with OAM modified GO was made using mini-emulsion method complimented by solvent evaporation technique. 3ml of GO-g-OA was mixed with 2ml of cobalt ferities (35 mg) in chloroform. These two were sonicated for 10 mins after it 50 ml of ultrapure water was added into it. This mixture was kept for sonication for 90 mins. This mixture after sonication was poured into pre-heated beaker at 70° C for solvent evaporation. Solvent was evaporated for 1 hour. After evaporation, centrifugation of the solution was performed to remove any contaminant. Centrifugation was performed at 4000 rpm for 60 mins (figure 3; step 3). As result of centrifugation brownish supernatant was saved and dried at 65° C.

### 3.5 Synthesis of APTMS coated CF

Bare CF nanoparticles were prepared using previously mentioned co-precipitation method without the presence of surfactant or coating polymer (Section 3.2). 95 mg of bare CF were taken and sonicated in ethanol for 1 hour. After sonication 2.5ml of 97% APTMS was added. This mixture was further kept for sonication for 1 hour. This step is of critical importance as the longer the time taken at this step will increase the risk of unwanted Silane polymerization. After the completion of sonication solution was washed twice in the presence of ethanol for 30 mins at 4000rpm. The pellet obtained was kept for drying at 45 ° C for 12 hours in vacuum oven.

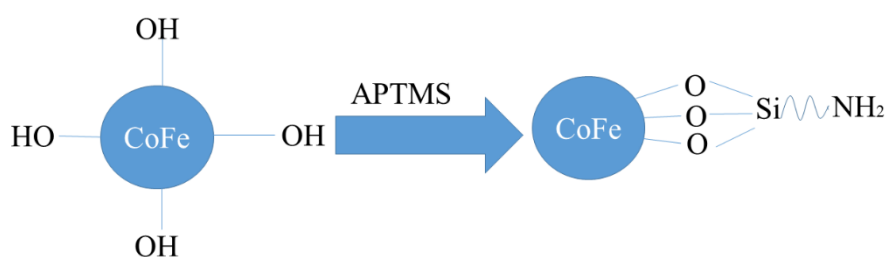


Figure 3.3 Schematic illustration of APTMS coating on bare CF

### 3.6 Covalent synthesis of GO-CF composite

A covalent composite between GO and APTMS modified CF was prepared. In this composite amine terminated CF nanoparticles were grafted to carboxylic free ends of GO. Thus leading to the formation of amide bond between GO and amine terminated

CF. 35 mg of GO and CF were completely dispersed in 50 ml of dimethylformamide (DMF) through sonication for 1 hour. An excess amount of catalyst N,N'-dicyclohexylcarbodiimide (DCC) (1.75g) was added. This mixture was stirred at room temperature for 48 hours. The resultant solution was washed and centrifuged (4000rpm for 20mins) with ethanol to remove unattached CF nanoparticles. The final solution was kept for drying at 60° C for 48 hours.

### 3.7 Analysis and characterization techniques used

#### 3.7.1 X-Ray diffraction analysis

##### Theory

X rays were discovered by W.C. Röntgen in 1895. These X rays are basically electromagnetic radiations with photon energy ranging from 100eV to 100 KeV. X rays have been employed for various applications such as X ray diffraction, X ray crystallography and X ray fluorescence spectroscopy. For X ray diffraction only X rays with shorter wavelengths are used (1KeV and 120 KeV). This is particularly so that these x rays become comparable to size of atoms thus help probing the structure and molecular arrangement of atoms and molecules in wide range of materials. X rays are generated using x ray tubes and synchrotron radiations. X rays are generated when focused electron beam is accelerated through high voltage field bombards a stationary and rotating solid target. This target emits a continuous spectrum of x rays which are known as Bremsstrahlung radiation. These high energy radiation also leads to the process of ionization of targeted solid atom. These high energy vacant shell spaces are filled by free electron upon which a x ray photon characteristics of target material is emitted. Common targets used in x ray tubes include Cu and Mo, which emit 8 keV and 14 keV x-rays with corresponding wavelengths of 1.54 Å and 0.8 Å respectively.

These x rays generated from the target upon interaction with sample material generates secondary diffracted beams of X-rays. These secondary diffracted beam of x rays is corresponding to interplanar spacing of crystalline structure obeying Bragg's law.

$$n\lambda = 2d\sin\theta$$

diffraction and  $\theta$  is the diffraction angle. Whereas Scherer formula is used to calculate size of the crystal lattice.

$$D_p = 0.94\lambda / (\beta \cos\alpha)$$

## **Experimentation**

XRD was used to investigate the crystal structure of the ferrites, graphene oxide and subsequently its composites. The X-Ray Diffraction STOE  $\theta$ - $\theta$  was used. Diffraction was performed for  $2\theta$  range from  $20^\circ$  to  $70^\circ$  degrees for ferrites while 5 to 55 for graphene oxide whereas composites were analysed between the ranges of  $5^\circ$  to  $70^\circ$  with step size of  $0.04^\circ$ . XRD pattern was further analyzed and compared with JCPDS library using X'Pert high score software.

### **3.7.2 Fourier Transform Infrared Spectroscopy (FTIR)**

#### **Theory**

FTIR spectroscopy is an idea based upon interference of radiations to yield interferogram. Later a signal is produced which is the function of change of pathlength between two beams. The domains such as distance and frequency are interconvertible by mathematical method of Fourier-transformation. The basic components of FTIR spectrometer includes source, interferometer, sample, detector, amplifier, analog-to-digital and computer. Radiation from the source is passed through an interferometer before reaching to the detector. High frequency contributions are eliminated by a filter. Afterwards data is converted to digital form from analog format. This digital data is transferred to computer where it is Fourier transformed.

#### **Experimentation**

A Fourier transform infrared spectrum was collected in transmittance mode on Perkin Elmer FTIR spectrometer. The scan of spectrum was run ranging from  $450\text{cm}^{-1}$  to  $4000\text{cm}^{-1}$ . Samples were dispersed and hydraulic pressed along KBr powder in a pellet form. Most common interferometer used in FTIR spectroscopy is Michelson interferometer.

### **3.7.3 Atomic Force microscopy (AFM)**

#### **Theory**

AFM generates a 3D image of a nanoscale surface. This image is created by measuring the forces between the probe tip and sample distance. The probe is supported on a cantilever. The tip of the probe smoothly touches the surface and records the small forces that exist between tip and the sample surface. AFM operates at three basic modes contact mode, non-contact mode and Tapping mode. AFM provides information such as topography of samples (thickness and roughness).

#### **Experimentation**

Sample dilutions were prepared and sonicated before a drop was placed on silica substrate. Drop was oven dried (60°C) to remove any moisture. All the images were recorded in tapping mode. Atomic Force Microscope JEOL (JSPM-5200) was used.

### **3.7.4 Ultraviolet Visible Spectroscopy (UV Vis)**

#### **Theory**

This absorption based spectroscopy employs the use of electromagnetic radiations ranging from 190-800 nm. This range is divided into ultraviolet region (190-400nm) and visible region (400-800 nm). The absorption of ultraviolet or visible radiation leads to energy level transition of molecules this way it is also known as electronic spectroscopy as well. UV Vis spectroscopy utilizes the principle of Beer-Lambert Law. This law states the fraction of light being absorbed is proportional to number of absorbing molecule in its paths. This means that the greater the number of molecules that absorb light, greater the extent of absorption and higher intensity peak is obtained in the absorption spectrum.

#### **Experimentation**

UV Vis spectra was recorded using diluted solutions of sample where solvent with lower wavelength cut off limits was used. Diluted samples were transparent. Range of spectra used was between 200-800 nm.

### **3.7.5 Testing for Peroxidase like activity (H<sub>2</sub>O<sub>2</sub> detection)**

In order to detect the presence of H<sub>2</sub>O<sub>2</sub> in the environment, TMB was employed as a chromogenic substrate for the peroxidase activity of the composite under this study. This TMB substrate after its oxidation gives blue colour which can be detected by the UV Visible spectrophotometer with maximum absorbance at 652 nm wavelengths. Range of temperature (20-60 ° C), pH (2-6) and concentration of composite (20µg/ml – 100µg/ml) were varied to study the optimal conditions and detection limit of the composite for H<sub>2</sub>O<sub>2</sub>. While in our experimentation we have used 2ml(0.2M) of sodium acetate (NaAc- HAc) buffer at (pH around 3), 15mM (20µl) of TMB with composite 80 µg/ml(10µl) for the detailed study of H<sub>2</sub>O<sub>2</sub> (5mM) detection limit unless otherwise stated. The process of oxidation of TMB by the composite was monitored at 652nm at 37° C.

## Chapter 4.

# Results and Discussion

### 4.1 Characterization of physical GO-CoFe composite

Here we present a simple, versatile and straightforward approach to anchor hydrophobic cobalt ferrites superparamagnetic nanoparticle on OAM modified GO to form water dispersible magnetic nanocomposite (Figure 4.1). The Physical composite of GO-CoFe was synthesized using GO sheets which were pre-modified using OAM. Oleic acid coated CoFe were decorated on pre-modified OAM-g-GO. OAM acted as a hydrophobic binder mediating the stabilization of hydrophobic CoFe on GO-g-OAM. Hydrophobic-hydrophobic interaction between OAM-g-GO and oleic acid CoFe leading to the formation of water dispersible magnetic nanocomposites (MNCs). This composite was characterized further for synthesized material characterization and its potential application in peroxidase mimetics (Figure 4.1). Physical composite of the similar nature has been synthesized and reported beforehand for biomedical applications such as hyperthermia and MRI application. However in this work few changes has been made to adopt the said procedure for synthesis.

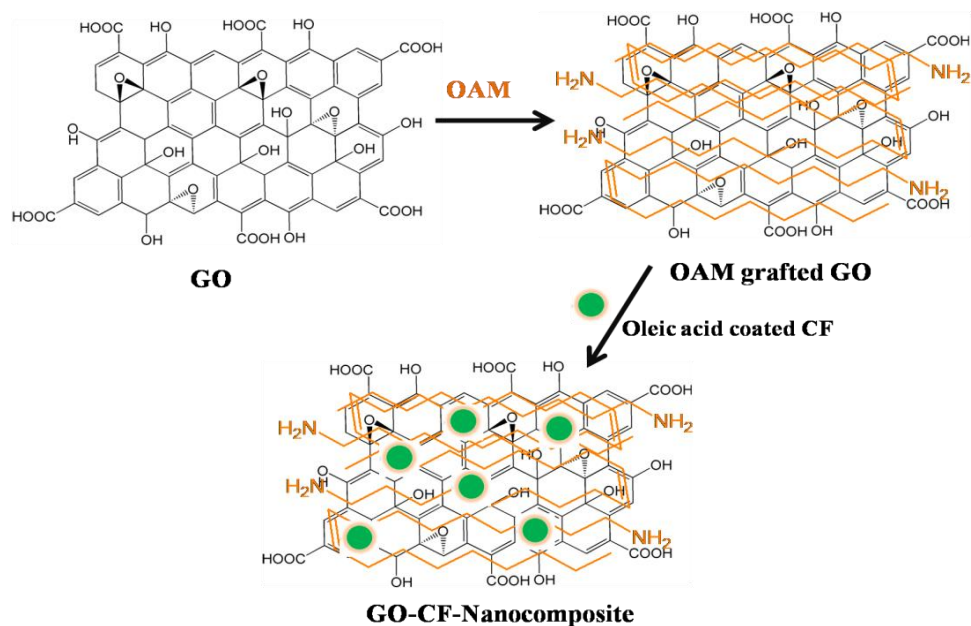


Figure 4.1 Schematic illustration of formation of physical GO-CoFe nanocomposites

GO-CF nanocomposite was prepared through physical coupling method i.e. mini-emulsion technique and was found to be water dispersible. For the characterization of GO-CF nanocomposite, various techniques such as XRD, UV-Vis spectroscopy, FTIR and SEM were used. X-ray diffractogram (Figure 4.2) showed an intense peak at an angle  $10.8^\circ$ , specific to GO (Figure 4.2a) where the d spacing represents the interplanar distance. This interplanar distance increases by increased trapping of oxygen atoms on the periphery. The obtained d spacing in this case was 0.80nm. There appears to be no un-oxidized graphite and reduced GO lattice peak in the diffractogram. Oleic acid coated CF was prepared using co-precipitation method which showed an expected pattern of inverse spinel structure and the pattern was in accordance with the cubic CF (JCPDS: no: 22-1086). It was observed that functionalization of ferrites did not cause degradation or phase shift of the parent CF (Figure 4.2b). The average crystallite size in this case was determined using Scherrer formula using first strongest peak. Presence of oleic acid serves as capping agent which helps reducing the size of nanoparticles by stopping the CF growth process and serving as a barrier for mass transfer. Therefore, oleic acid provides a crucial role in maintaining the uniform and small size of CF. Presence of oleic acid has no effect on the structure and composition of CF since no impurity was detected using XRD. Presence of oleic acid not only prevents CF particles aggregation but also provides a platform for their further functionalization. GO-CF composites showed CF crystallite representative XRD peaks (Figure 4.3c) but not GO

specific peak which is partly due to the presence of small amounts of GO in composite formation and partly because of the presence of large amounts of OAM which leads to the disappearance of GO specific peak as explained in an earlier work in detail[154]. It is to be noted that the combination of oleic acid and OAM is one of the most well reported combination of surfactants for controlled synthesis and stability of the nanocrystals. This combination is found to be effective in maintaining various functions of inorganic crystals. Some of these functions are magnetic, optical and catalytic[155].

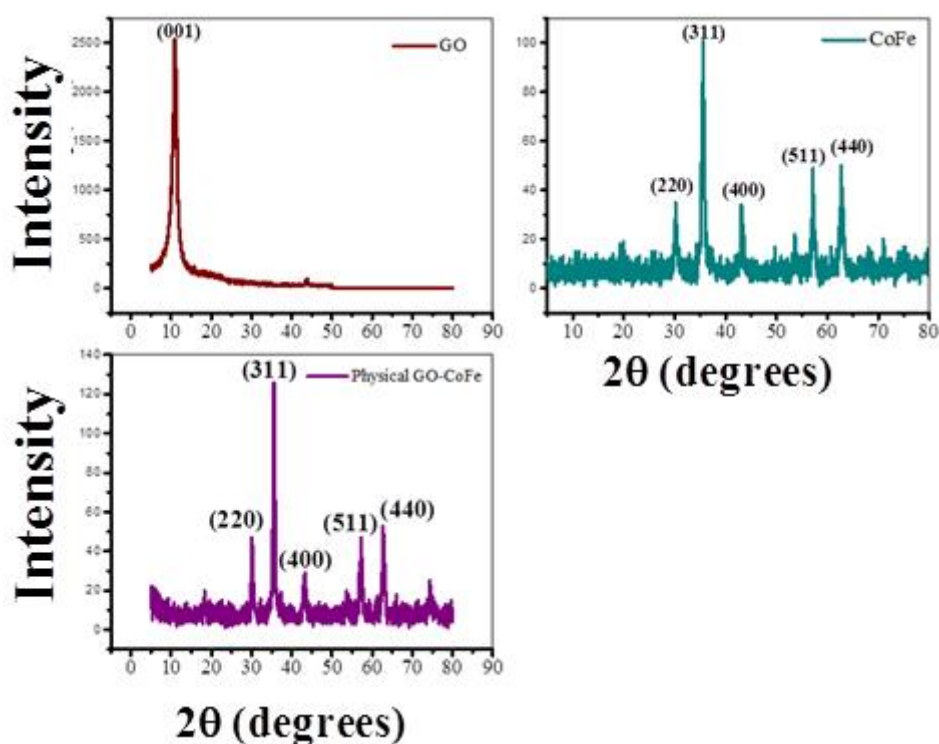


Figure 4.2 XRD pattern of (a) GO (b) Oleic acid coated CoFe and (c) physical GO-CoFe nanocomposite

Similarly, UV-Visible spectrum of GO exhibited distinct peak around 227nm (Figure 6a) which can be correlated with  $\pi$ - $\pi$  electronic transition in carbon atoms. This peak indicates the presence of highly oxidized graphene oxide. Furthermore, UV-Vis spectrum of GO-CF nanocomposite showed a minor hump around 250-300 nm (Figure 4.3), indicative of  $n$ - $\pi^*$  electronic transition incorporating carbon and oxygen atoms. Therefore, measured spectrum confirms the presence of highest absorbance at 227 nm and also establishes no red shift peak for GO-CF nanocomposite.

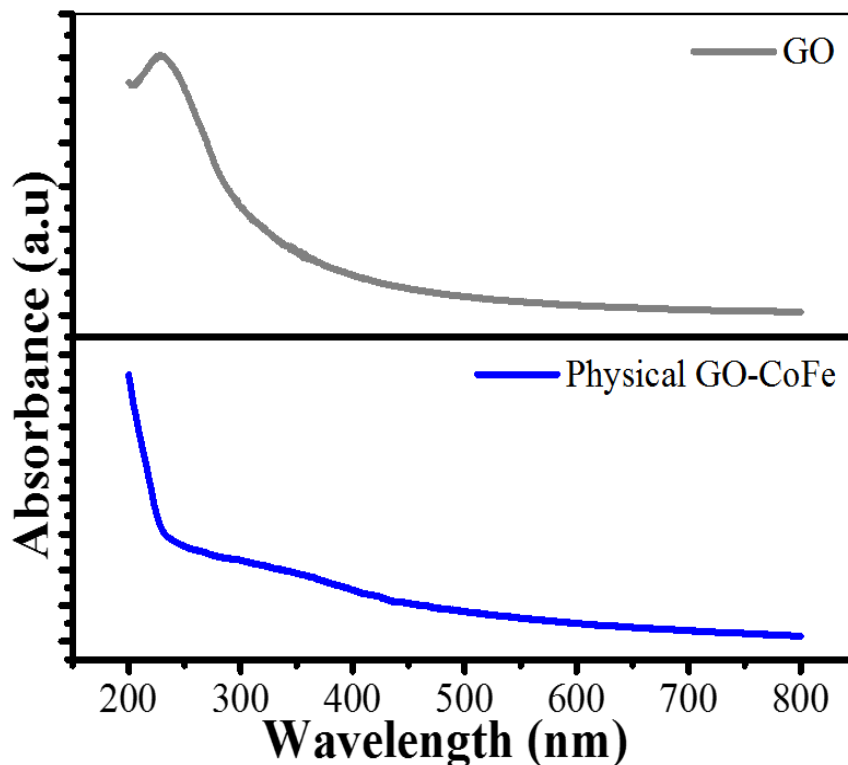


Figure 4.3 UV vis spectra of (a) GO (b) physical GO-CoFe nanocomposite

To visualize the morphology of CF, GO and composite, SEM images were recorded. SEM micrographs showed exfoliated layers of GO which were transparent and wrinkled (Figure 4.4 a) and lateral dimensions shown were very thin. Detailed analysis of GO sheets was carried out using AFM. Lateral dimensions of GO vary with oxidation process followed. Role of heterogeneous oxidation has been reported previously in detail [16, 156]. Particle size, shape and structure of CF were elucidated using SEM micrographs which indicated homogenous dispersion of particles without any significant agglomeration. The shape of the particles was found to be uniformly spherical (Figure 4.4 b) and the average particle size was found to be 15nm for the oleic acid coated CF NPs. The size shown by SEM was in agreement with the size determined by Scherrer's equation using the two most intense peaks. In the case of GO-CF nanocomposite, CF NPs were well dispersed on GO matrix without altering the morphology of the CF (Figure 4.4 c). GO was surface modified using OAM in quantity sufficient enough to promote a hydrophobic-hydrophobic interactions between GO and oleic acid modified CF[17]. While the excessive OAM was washed out during centrifugation, oleylamine modified GO not only promotes an interaction between GO and CF but also makes water dispersible nanocomposite. OAM modified GO helps to maintain excellent dispersity of CF on GO sheets. The crystallinity of CF NPs in

nanocomposite was maintained as indicated by the XRD spectrum of nanocomposite. Role of OAM on maintaining the uniform distribution of CF NPs on GO was also elucidated by using a relatively small amounts of OAM. Presence of OAM in negligible amounts led to the aggregated distribution of CF (Figure 4.4 d). It is assumed that OAM as intermediary binder enhances the colloidal stability of the composite. Good colloidal stability is of fundamental importance for biomedical applications [20] and maintaining colloidal stability continues to be an issue for ferrite decorated GO composites due to various reasons. Through our demonstrated approach, we could overcome this problem effectively which lead to better colloidal stability.

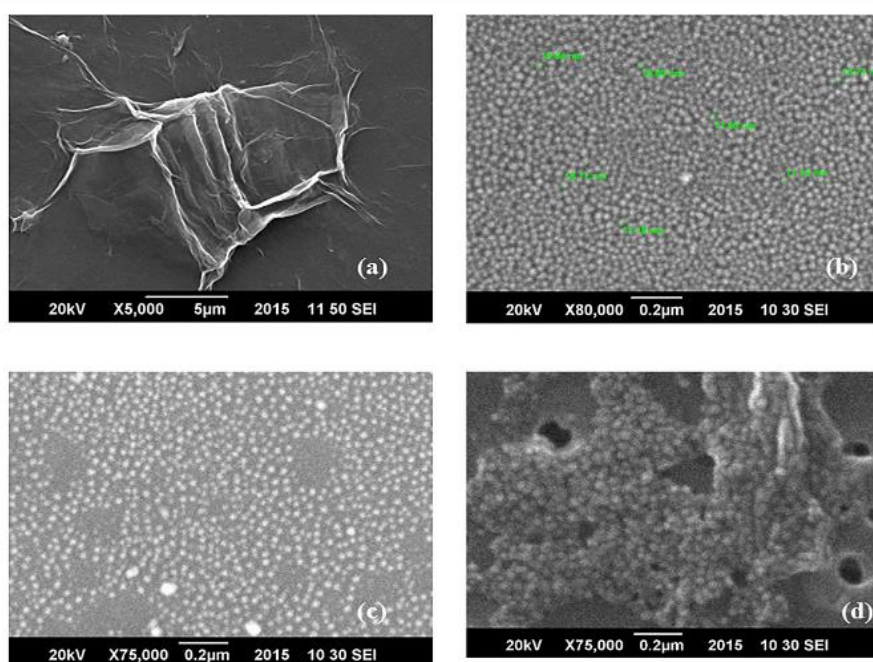


Figure 4.4 SEM micrograph of GO (a), CoFe (b), GO-CoFe (c, d) nanocomposite with varying amount of OAM.

FTIR spectrum gives a semi-quantitative analysis of the chemical bonds which are sensitive to the infrared wavelength. In case of physical GO-CoFe IR spectrum of GO shows a significantly sharp peak around  $3399\text{cm}^{-1}$  corresponds to OH stretching vibrations while peak at  $1628\text{ cm}^{-1}$  can be correlated to the  $\text{sp}^2$  hybridized  $\text{c}=\text{c}$  bonds. Peaks of epoxy (C-O) and hydroxyl (C-OH) groups can be seen at  $1243\text{cm}^{-1}$  and  $1401\text{cm}^{-1}$  respectively. Modification of GO-g-OAM was also confirmed through FTIR spectrum indicating disappearance of peaks due to epoxide stretching vibrations (around  $1120\text{ cm}^{-1}$ ) due to coupling of amine of OAM to the epoxy group of GO. In this case, appearance of amide bond was confirmed by the subsequent appearance of  $-\text{C}-\text{N}-$

stretching around  $1465\text{cm}^{-1}$ . Additionally, characteristic peaks of OAM can also be seen at  $720\text{ cm}^{-1}$ ,  $966\text{ cm}^{-1}$  and  $2911\text{cm}^{-1}$  for  $-\text{CH}_2$  bending vibrations,  $=\text{CH}_2$  bending vibrations and  $-\text{CH}_2$  symmetric and asymmetric stretching vibrations respectively (Figure 4.5). FTIR spectrum of oleic acid coated CF shows the appearance of high frequency peak at  $584\text{ cm}^{-1}$  which is the characteristic peak for Fe-O bond vibration. Peaks around  $1431\text{cm}^{-1}$  are characteristic for symmetric and asymmetric vibrations of  $-\text{COO}$  groups. Vibration of  $-\text{CH}_2$  symmetric and asymmetric groups are represented through a sharp peak around  $2919\text{ cm}^{-1}$ . This peak is found to be characteristic of oleic acid coating [73]. FTIR spectrum of GO-CF nanocomposite contains peak at  $593$  unlike parent GO or GO-g-OAM spectra which indicates the incorporation of Fe-O groups to GO-g-OAM. Additionally, disappearance of epoxy peak around  $1243\text{cm}^{-1}$  could presumably be due to the participation of  $-\text{COOH}$  peripheral groups during nanocomposite formation. Peak around  $1636\text{ cm}^{-1}$  represents the skeletal migration of graphene nanosheets and also  $-\text{NH}-$  bending vibrations due to GO-g-OAM formation

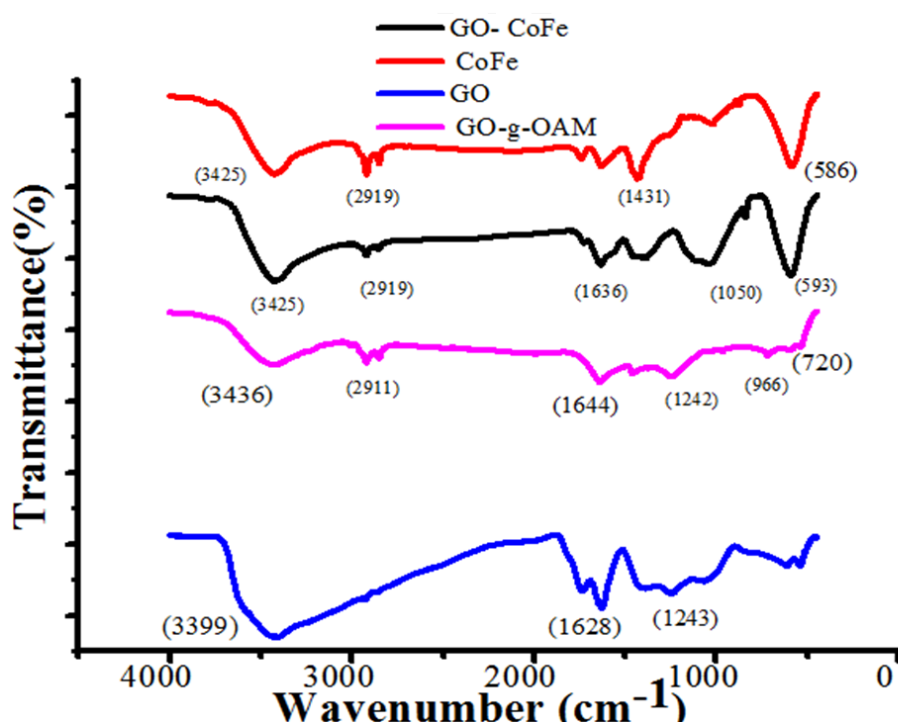


Figure 4.5 FTIR spectra of GO, GO-g-OAM, CoFe and physical GO-CoFe nanocomposite.

#### 4.2 Detection of Peroxidase like activity of physical GO-CoFe composite.

GO-CF nanocomposite synthesized by mini emulsion method was found to be water dispersible which led to the formation of a ferrofluid with enhanced colloidal stability. Chromogenic substrate (TMB) in the present investigation was used to demonstrate

peroxidase like activity of GO-CF nanocomposite in the presence or absence of  $H_2O_2$ . In this case, TMB +  $H_2O_2$  in the absence of GO-CF nanocomposite was found to be colorless while TMB+ $H_2O_2$  in the presence of GO-CF formed deep blue color. Appearance of deep blue color indicates the presence of oxidized form of TMB due to peroxidase like catalytic activity of GO-CF (Figure 4.6a).

Peroxidase mimetic catalytic activity of GO-CF nanocomposite was investigated in order to explore optimal conditions for the performance of new composite. Therefore, UV-Vis spectra of TMB and acetate buffer were recorded between 400 to 800 nm range. It was observed that TMB in the presence and absence of  $H_2O_2$  exhibited no strong/significant peak around 652 nm which is specific wavelength for the appearance of oxidized form of TMB. Furthermore, since peroxidase activity of GO as well as of CF is already known, we have investigated their peroxidase activity in order to compare the results with the activity of our nanocomposite material. Therefore, results obtained showed that peroxidase activity of our GO-CF nanocomposite was quite high in comparison to such activity for individual components which could be due to the synergistic effect of the components in our nanocomposite system (Figure 4.6b).

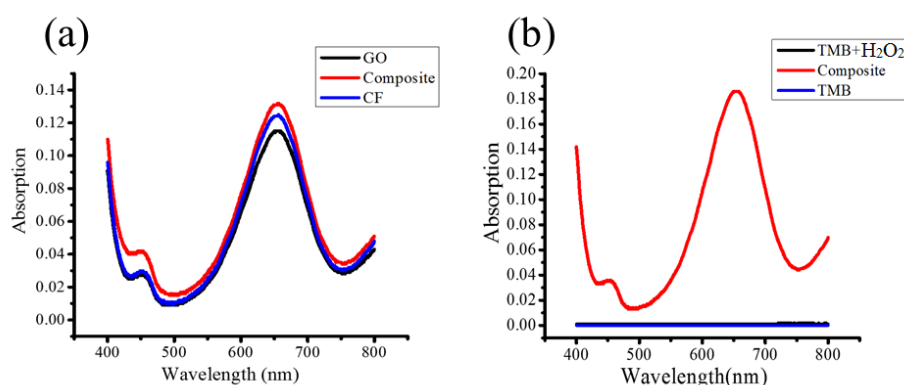


Figure 4.6 UV Vis spectra of (a) comparison of peroxidase activity of GO, CF and GO-CF nanocomposite and (b) TMB, TMB+  $H_2O_2$  and physical GO-CoFe nanocomposite

In order to investigate on the effect of the acidity of acetate buffer and the effect of temperature, various pH and temperature ranges were tested which showed that peroxidase activity of the catalyst was maximum at 3 pH and 40 °C (Figure 4.7 a and b).

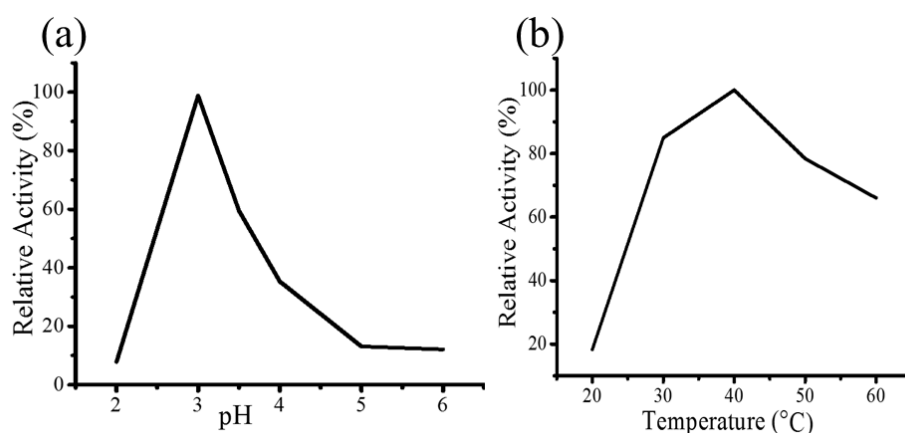


Figure 4.7 Relative activity of physical GO-CoFe at various pH (a) and temperature (b).

The effect of the concentration of GO-CF nanocomposite on the peroxidase like activity was also investigated which showed that by increasing the concentration of GO-CF nanocomposite from 20 $\mu$ g/ml-100 $\mu$ g/ml, increase in peroxidase like activity was observed (Figure 4.8). The observed behaviour of GO-CF nanocomposite was similar to what has already been reported for HRP enzyme. It is also worth noting that maximum activity of GO-CF nanocomposite around pH 3 eliminates the possibility of iron ion leaching which may lead to pseudo peroxidase like activity. Concentration of oxidized TMB product responds linearly to the increased concentration of GO-CF nanocomposite. Since CF is reported to contain reactive sites for H<sub>2</sub>O<sub>2</sub> adsorption and oxidation [144], our results are consistent with the previously reported studies where this effect can be attributed to the increased reactive sites available for the peroxidase like catalytic activity of GO-CF nanocomposite.

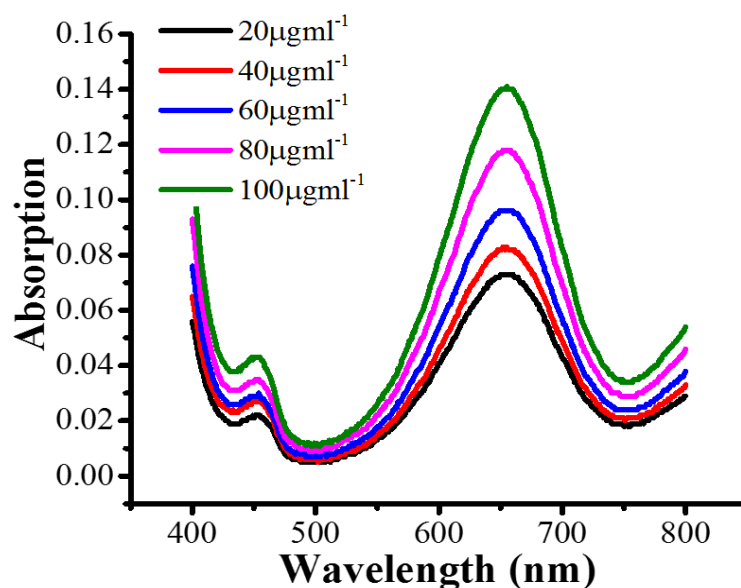


Figure 4.8 Dependence of peroxidase like activity on varying concentration of physical GO-CoFe composite (20-100µg/ml).

In order to develop a colorimetric method for the detection of  $\text{H}_2\text{O}_2$  by using inorganic enzyme,  $\text{H}_2\text{O}_2$  concentration was varied from 5 to 300  $\mu\text{M}$ . It was observed that higher concentration of  $\text{H}_2\text{O}_2$  did cause an inhibitory effect on the catalytic activity of the nanocomposite. The linear range of  $\text{H}_2\text{O}_2$  under optimal condition was found to be between 5 to 100  $\mu\text{M}$  with the limit of detection as 0.399  $\mu\text{M}$  (Figure 4.9). LoD estimated in the present case is comparable to previously reported graphene based nanocomposites such as  $\text{Co}_3\text{O}_4$ -rGO, Pt or Pd-rGO, CF-rGO,  $\text{Fe}_3\text{O}_4$ -GO where LoD reported was in the range from 0.3  $\mu\text{M}$ -5.3  $\mu\text{M}$  [133, 157-159].

#### Mechanism of peroxidase like activity of GO-CF nanocomposite

Peroxidases are oxidoreductase family in which peroxides such as  $\text{H}_2\text{O}_2$  or alkyl hydroperoxide (ROOH) is reduced where redox substrate (TMB) acts as an electron donor and is oxidized (Scheme 1).



**Scheme 1.** Schematic representation of peroxidase like activity

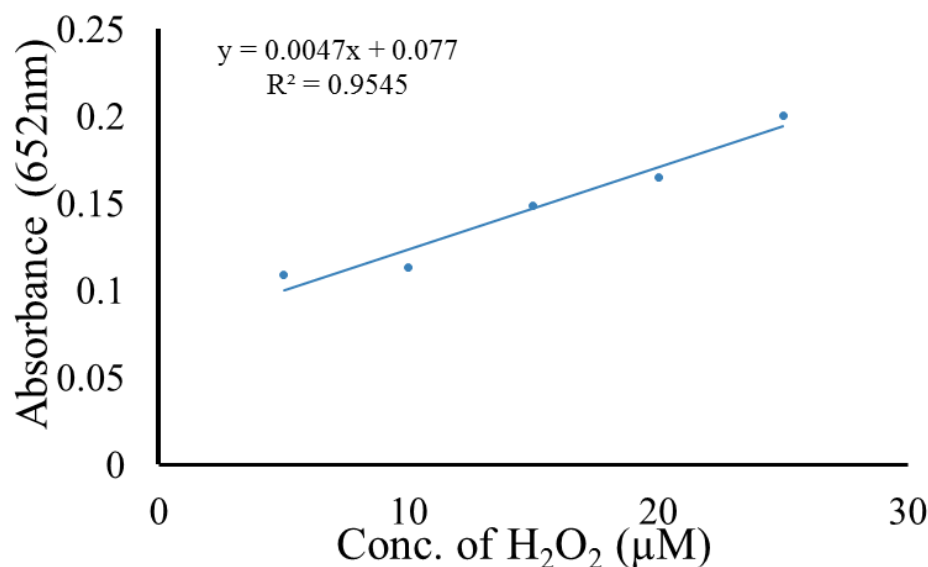


Figure 4.9 Linear calibration plot for H<sub>2</sub>O<sub>2</sub> detection using physical GO-CoFe nanocomposite.

Magnetic nanocomposites such as GO-CF nanocomposite carries out peroxidase like activity where CF binds to H<sub>2</sub>O<sub>2</sub> and generate hydroxyl ions. These hydroxyl ions further carry out oxidation of TMB into blue colour product namely 3,3',5,5'-tetramethylbenzidine diimine (TMBDI). This is how the presence of peroxides can be detected colorimetrically by employing various chromogenic substrates such as TMB. Additionally, presence of Co<sup>+2</sup> ions in the nanocomposite favours the decomposition of H<sub>2</sub>O<sub>2</sub> into hydroxyl free radical and hydroxyl ion which further enhance the oxidation of TMB.

Furthermore, GO in nanocomposite, due to high surface area, facilitates the adsorption affinity for organic substrate such as TMB through  $\pi$ - $\pi$  and hydrophobic interaction [139]. Therefore, enhanced peroxidase activity of the nanocomposite is due to the synergistic effect of both CF as well as of GO. Such materials show potential for the differential and colorimetric detection of cancer cells in the living environment through detecting the presence of reactive oxygen species.

We have demonstrated for the first time peroxidase like activity of GO-CF nanocomposite prepared through physical linkage. This nanocomposite showed better colloidal stability. The adopted approach for the synthesis of nanocomposite could potentially lead to less cytotoxic materials and could provide viable options for theranostic applications. We achieved uniform distribution of CF nanoparticles on GO sheets with the help of OAM which acts as binder. We were also able to demonstrate that when OAM was grafted on GO in negligible amounts, poor dispersion of CF was

obtained which resulted in poor peroxidase like activity of GO-CF nanocomposite (MNC-1) as shown below (Figure 4.10).

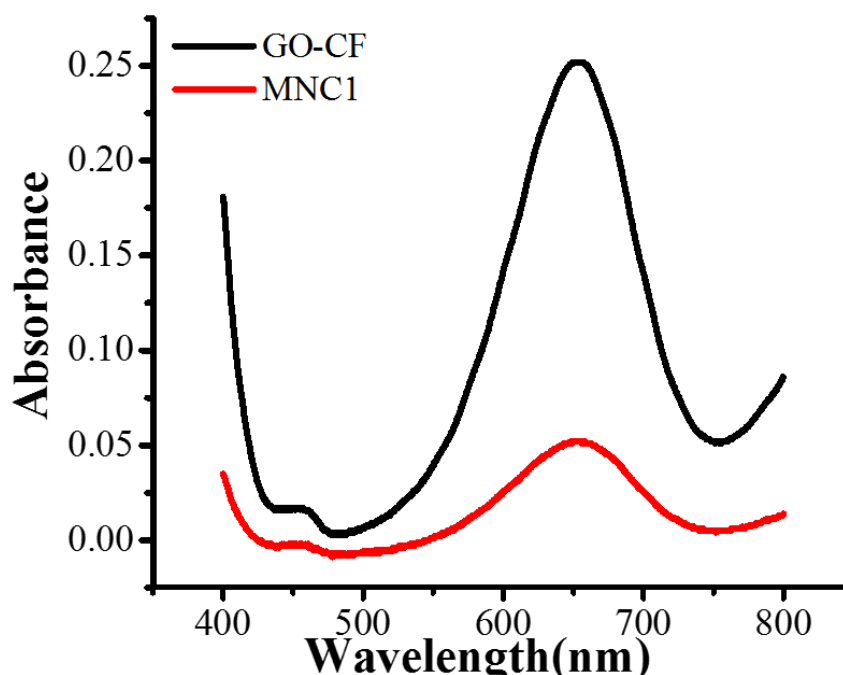


Figure 4.10 Dependence of peroxidase activity by varying CoFe NPs on GO sheets

### 4.3 Characterization of covalent GO-CoFe composite

Here we have created a covalent composite using a facile three step method. Covalent composite is having amide bond between two combined materials (GO-CoFe). In this work CoFe were synthesized using co-precipitation method, these CoFe were post modified using 3-Aminopropyl trimethoxy silane (APTMS). Post modification of CoFe with APTMS results in presence of amine ( $\text{NH}_2$ ) groups GO was synthesized using improved hummer's method. The obtained GO sheet was nanosized in size. This nanosheet of GO contains functional groups such as carbonyl, carboxyl, epoxide and hydroxyl groups. Carboxyl groups of GO reacted with amine groups of APTMS coated CoFe. Catalyst such as DCC was used as an acid activator for the synthesis amide bond [160, 161] Carboxyl groups of GO sheets act to tether amine terminated CoFe particles on itself. Schematic diagram of adopted synthesis method is illustrated in detail (Figure 4.11).

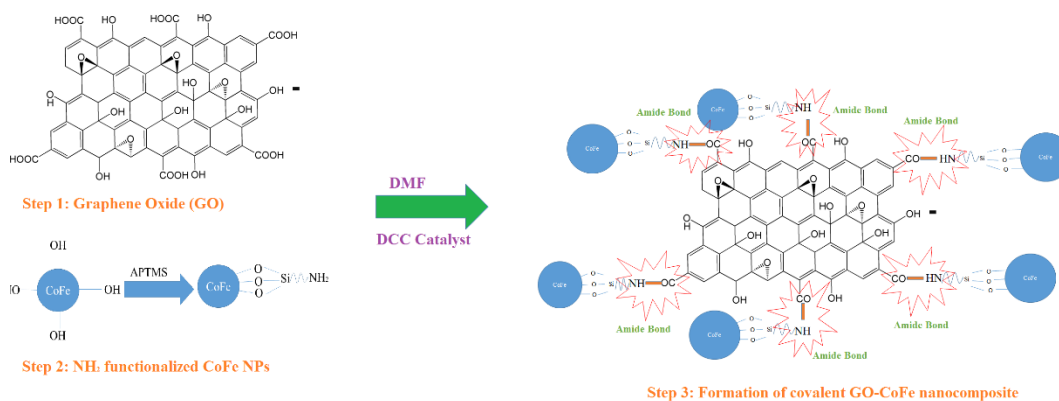


Figure 4.11 Schematic illustration of formation of covalent GO-CoFe nanocomposite via amide linkage.

This method of synthesis of GO based magnetic composite has been reported by using various techniques and for other applications. Whereas polymer such as APTS has been one of the most abundantly used polymer for ferrites modification. Use of such ferrites has been explored in the field of enzyme mimetics, microwave absorption, hyperthermia and MRI [57, 84, 112].

Characterization of covalent GO-CoFe composite was carried using XRD, FTIR, SEM and UV Vis spectroscopy. XRD analysis of GO revealed presence of highly oxidized peak at  $10.8^\circ$  with interplanar distance of 8 nm. Peak of GO corresponds to lattice plane 001 in contrast to 002 plane of graphite flakes. Bare CoFe nanoparticles were characterized using XRD. Their XRD diffractogram indicates presence of highly crystallite structure with characteristic of cubic spinel structure which was in accordance with standard JCPDS card 22-1086. Upon testing APTMS coated CoFe it was seen that there was no degradation in CoFe particles thereby it was exhibiting diffractogram similar to bare CoFe nanoparticles. However it is to be noted that by the addition of APTMS diffraction maxima becomes weaker and broader [73]. Upon analyzing the XRD retrieved pattern, size of bare and APTMS coated CoFe was determined using Scherrer's equation (Figure 4.12). The size of bare CoFe particle was found to be 14 nm in contrast to APTMS coated CoFe nanoparticles with size 17 nm. The increase in particle size was observed due to the APTMS coating.

Covalent composite of GO-CoFe XRD diffractogram indicated the presence of cubic spinel structure of CoFe with its characteristic peaks in the synthesized materials.

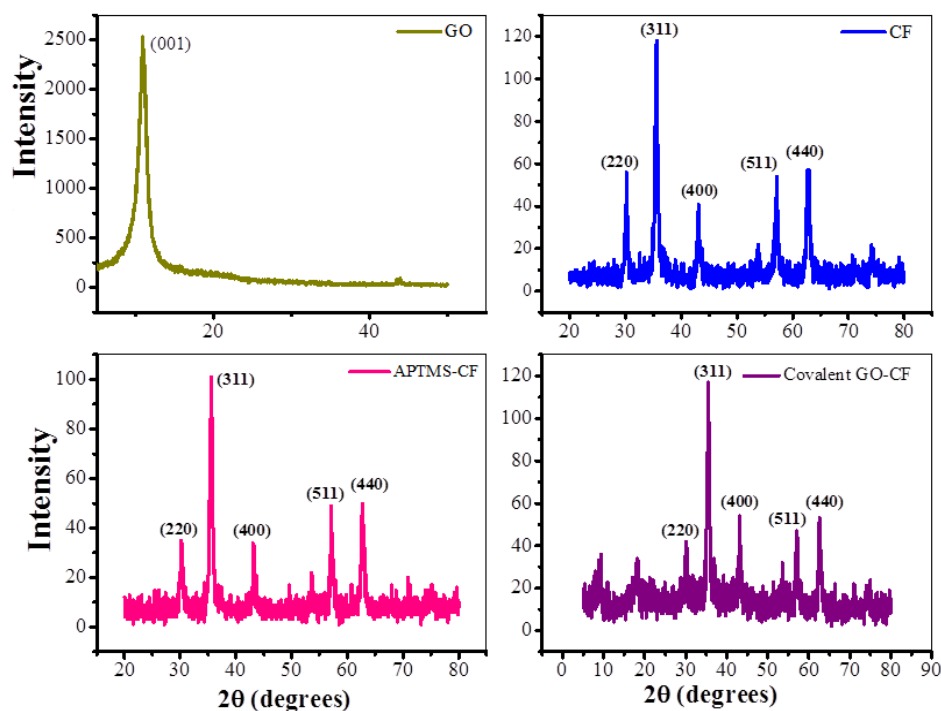


Figure 4.12 XRD spectra of a) GO b) CoFe c)CoFe-APTMS d) GO-CoFe covalent composite nanocomposites.

UV-Vis spectra of synthesized GO and covalent GO-CoFe indicates presence of highly oxidized structure with a dominant peak around 227 nm. In contrast to GO, covalent composite of GO-CoFe has a small hump around 260 nm. This corresponds to the partial reduction of GO (Figure 4.13).

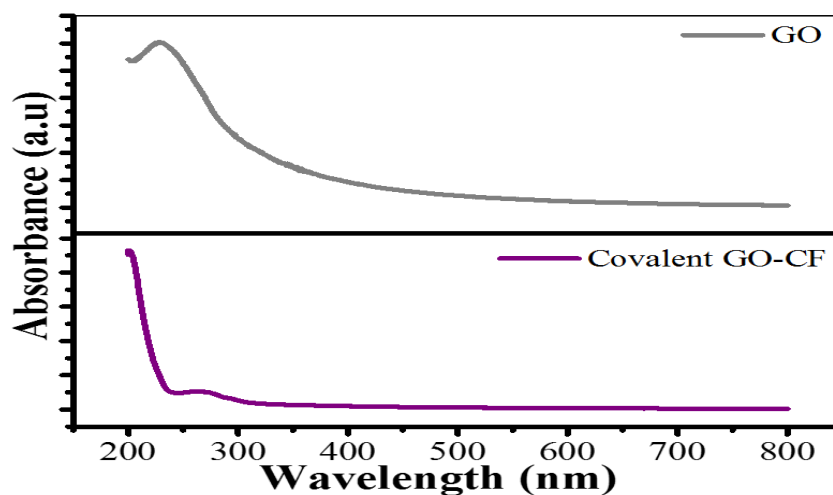


Figure 4.13 UV Vis spectrum of a) GO and b) GO-CoFe covalent nanocomposites.

SEM micrographs of GO, bare CoFe and APTMS coated CoFe exhibits presence of thin sheet of GO obtained from oxidation of graphite flakes and repeated washing. CoFe

nanoparticles are roughly spherical structure with increase in size formation (Figure 4.14). Whereas covalent GO-CoFe composite showed presence of nanoparticles anchored to the GO sheets. These nanoparticles are spherical in structure however few of the CoFe were present in the form of free CoFe nanoparticles in the solution. This may be due to their failure to participate in formation of amide bond between GO-CoFe.

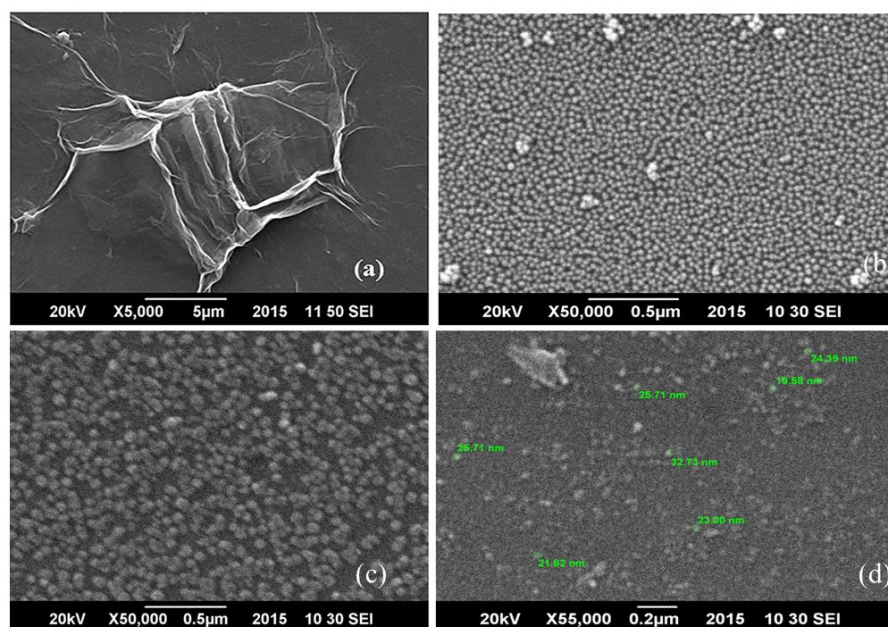


Figure 4.14 SEM micrographs of a) GO b) CoFe c)CoFe-APTMS and d) GO-CoFe covalent nanocomposites.

In case of covalent GO-CoFe IR spectrum of GO shows a significantly sharp peak around  $3399\text{ cm}^{-1}$  corresponds to OH stretching vibrations while peak at  $1628\text{ cm}^{-1}$  can be correlated to the  $\text{sp}^2$  hybridized  $\text{C}=\text{C}$  bonds. Peaks of epoxy (C-O) and hydroxyl (C-OH) groups can be seen at  $1243\text{ cm}^{-1}$  and  $1401\text{ cm}^{-1}$  respectively. CoFe nanoparticles shows a characteristic peak at  $585\text{ cm}^{-1}$  which is attributed to stretching vibrations of oxygen and cations ( $\text{Fe}^{+2}$ ) at octahedral and tetrahedral positions confirming the formation and presence of CoFe nanoparticles (Figure 4.15). Peak at  $1025\text{ cm}^{-1}$  attributes to the SiO-H and Si-O-Si bonds in addition to this a weak band at  $880\text{ cm}^{-1}$  corresponds to  $\text{HN}_2$  groups in CoFe-APTMS. Peak at  $1619\text{ cm}^{-1}$  corresponds to  $\text{C}=\text{O}$  bonds for CoFe-APTMS nanoparticles Whereas peaks at  $3427\text{ cm}^{-1}$  and  $2927\text{ cm}^{-1}$  reflects the presence of  $-\text{OH}$  and  $\text{C-H}$   $\text{sp}^3$  stretching vibrations. In MNC-11 (GO-CoFe covalent nanocomposite) nanocomposite has a characteristic peak  $1630\text{ cm}^{-1}$  with a blue shift. This peak indicates the amide and carbonyl stretching. This blue shift point at peak  $1630\text{ cm}^{-1}$  not only indicates the skeletal change in structure of GO but also

confirms the formation of new amide bond leading to the formation of covalent bond between GO-CoFe nanocomposites.

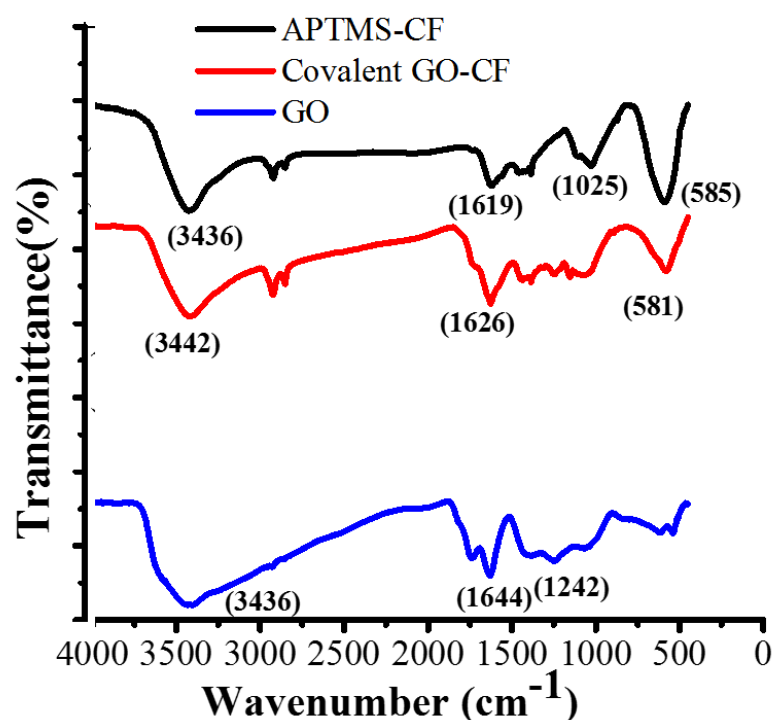


Figure 4.15 FTIR spectrum of GO, CF-APTMS and covalent GO-CF nanocomposites.

Observation of SEM was confirmed using AFM topographic analysis. AFM of GO sheet indicates the presence of heterogeneously thin sheet of GO with average thickness of around 5nm. Thus the lateral dimension of GO indicates the presence of single layer GO sheet. In contrast to GO, covalent GO-CoFe nanocomposite indicates the presence of spherical ferities on GO sheets. Through this AFM topographic image of GO-CoFe it was seen that APTMS coated CoFe were uniformly distributed over GO sheet with average height of around 39 nm (Figure 4.16).

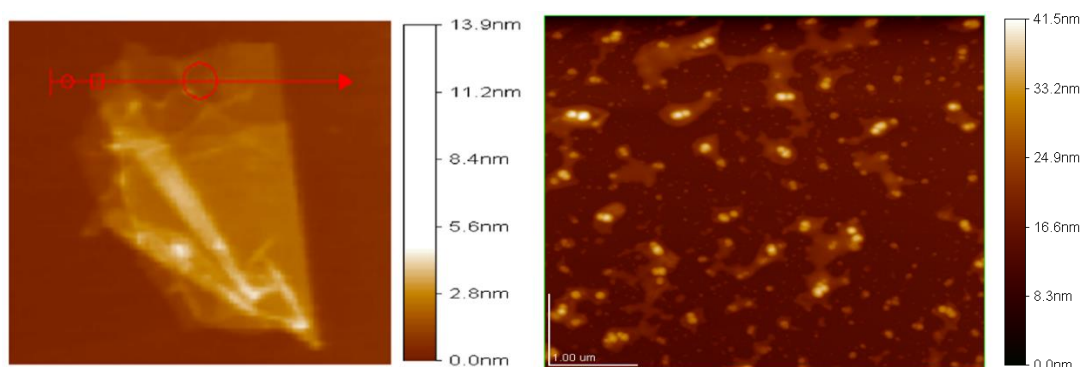


Figure 4.16 AFM analysis of GO(a) and GO-CF (b) covalent nanocomposites.

#### 4.4 Detection of peroxidase activity of covalent GO-CoFe composite

GO and CoFe both are known for their potential as peroxidase mimetic material. However neither the use of covalent GO-CoFe composite nor the use of APTMS coated CoFe has been tested for enzyme mimetics. This is the first time amide bond based covalent GO-CoFe nanocomposite was tested for its peroxidase potential. In order to do so GO-CoFe nanocomposite was compared to the GO, and APTMS coated CoFe nanoparticles. It was established that the GO-CoFe nanocomposite had better catalytic activity compared to GO and APTMS coated CoFe nanoparticles alone. In addition to this it was demonstrated through the use of UV-Vis spectra that  $\text{H}_2\text{O}_2 + \text{TMB}$  and TMB alone had no contribution to the characteristic spectra of peroxidase activity of GO-CoFe covalent nanoparticles (Figure 4.17).

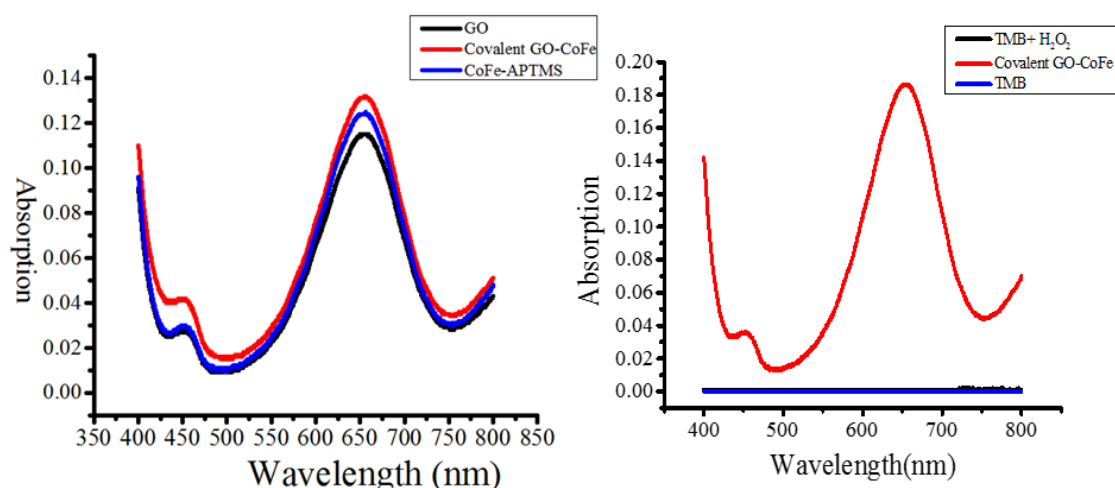


Figure 4.17 UV Vis spectra of (a) comparison of peroxidase activity of GO, CoFe-APTMS and covalent GO-CoFe nanocomposite and (b) TMB, TMB+  $\text{H}_2\text{O}_2$  and Covalent GO-CoFe nanocomposite

Behaviour of GO-CoFe nanocomposite over a specified range of temperature and pH. It was established that GO-CoFe nanocomposite had optimum peroxidase activity at pH 3 (Figure 4.18). Whereas GO-CoFe nanocomposite peroxidase activity increased upon increase in temperature.

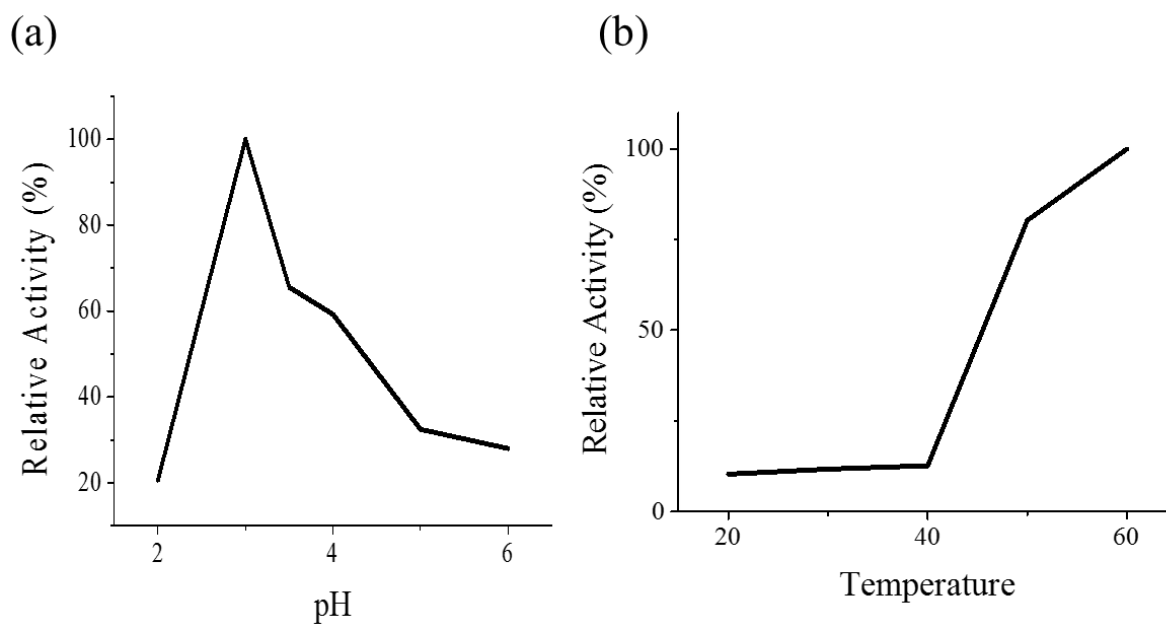


Figure 4.18 Relative activity of covalent GO-CoFe covalent nanocomposite a) pH and b) Temperature

With increase in concentration of the catalyst increase in peroxidase like activity was observed. This is effect is due to increase in catalytic sites present for the peroxidase reaction, where maximum amount of  $H_2O_2$  is absorbed and help to produce peroxides leading to oxidation of TMB substrate into oxidized colour product TMBDI (Figure 4.19).

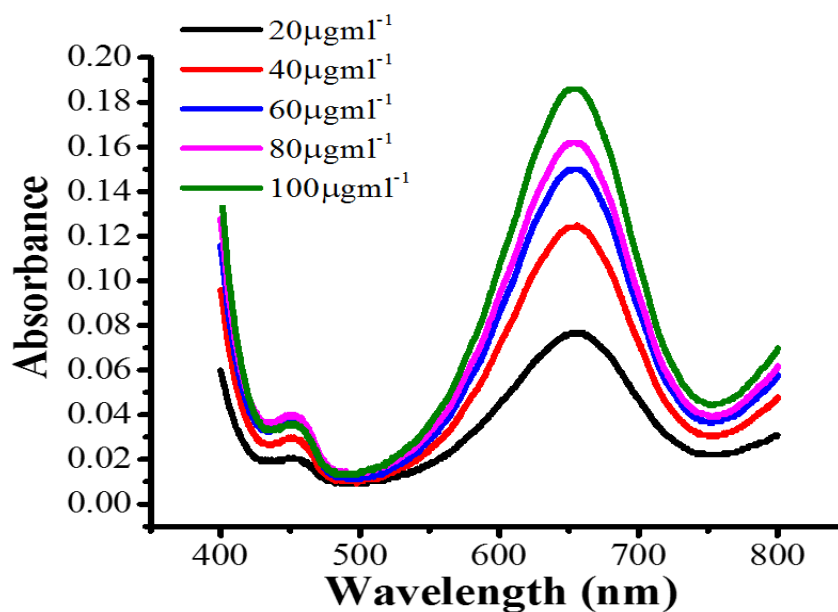


Figure 4.19 Effect of increase in concentration of covalent GO-CoFe nanocomposite.

In order to find LoD of GO-CoFe covalent nanocomposite calibration curve for H<sub>2</sub>O<sub>2</sub> was made (Figure 4.20). This calibration indicates the LoD of this nanocomposite as 0.55 μM.

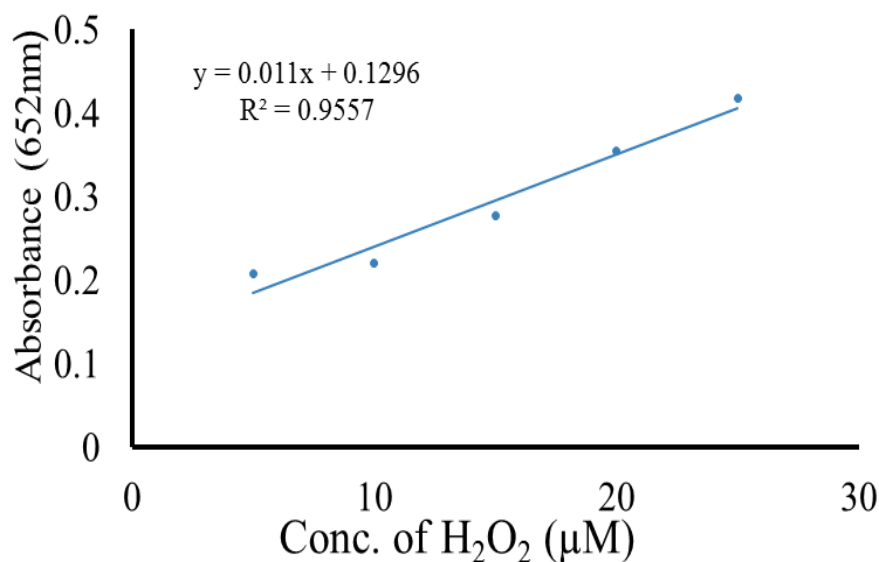


Figure 4.20 Linear calibration plot for H<sub>2</sub>O<sub>2</sub> detection using covalent GO-CoFe nanocomposite

On comparing both the composites following conclusions were drawn. Physical GO-CoFe nanocomposite is less time consuming process. The stability physical GO-CoFe nanocomposite collide was long lasting approximately colloidal solution was stable for 4-6 weeks. Whereas dispersion of nanoparticles on GO sheets was more uniform than the CoFe-APTMS nanoparticles covalently tethered to GO sheets. Use of catalyst in case of covalent GO-CoFe nanocomposite will result in increase in the cost of nanocomposite formation. In addition to this DCC use leads to the production of water insoluble byproducts during amide bond formation which needs to be removed additional (Table 4.1). Covalent GO-CoFe nanocomposite are stable over a range of pH and temperature. This is due to the fact the covalent bond formation make it less prone to environmental changes than the physically linked composites. Physical composite showed improved LoD for H<sub>2</sub>O<sub>2</sub> than the covalent GO-CoFe nanocomposite. Improved LoD of physical GO-CoFe nanocomposite is attributed to uniform dispersion of CoFe nanoparticles on GO sheets. In addition to this physical linkage between GO-CoFe nanoparticles allows abundant space for oxidoreductase activity of GO-CoFe nanocomposite. Whereas a large amount of TMB is adsorbed by the GO and CoFe nanoparticles surface.

Table 4.1 Brief tabulated comparison of properties of physical and covalent GO-CoFe nanocomposite.

<b>Properties</b>	<b>Physical GO-CoFe nanocomposite</b>	<b>Covalent GO-CoFe nanocomposite</b>
Less time for processing	Present	
Control over chemistry	Present	
Colloidal Stability	Present	
Use of Catalyst		Present
Better dispersion	Better	
Better Catalytic Activity	Present	
Stability over pH and Temperature		Present
Limit of detection	Present, improved	

## Chapter 5

### Conclusion and future recommendations

In the research work carried out under this project two types of magnetic composites were synthesized, one was physical GO-CoFe NP composite while another was covalent composite achieved using amidation reaction between carboxyl groups of GO and amine groups of APTMS CoFe nanoparticles. Both of these composites were synthesized, characterized while their further potential for enzyme mimetic activity was elucidated. Proposed mechanism of physical/covalent GO-CoFe nanocomposites is illustrated for colorimetric detection of cancer cells (Figure 5.1). GO-CoFe nanocomposite (a) will bind to the cancer cells (c) selectively in contrast to healthy cells (b). In cancer cells presence of  $H_2O_2$  and TMB will lead to colorimetric change in the cellular suspension leading to their differential detection (e). In this protocol, selective attachment of GO-CF nanocomposite to cancer cells can be enhanced using cancer specific receptors such as folate receptors.

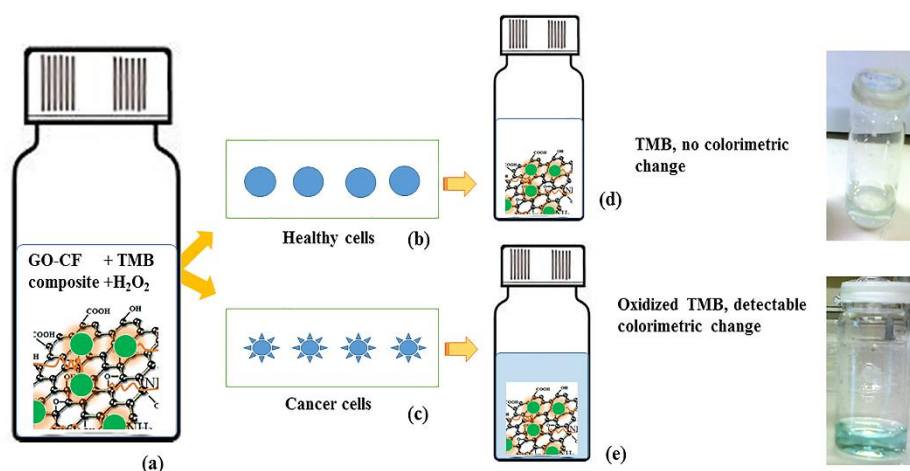


Figure 5.1 Schematic illustration of proposed cancer cell detection using physical/covalent GO-CoFe nanocomposite.

In physical composite study, oleic acid CF NPs were decorated on GO through OAM as mediator resulting in water dispersible nanocomposite. We achieved uniform distribution of CF NPs on GO sheet while maintaining their morphology and structure. This water dispersible nanocomposite exhibited stable and effective peroxidase like

activity for  $\text{H}_2\text{O}_2$  detection. In comparison to natural enzymes, this nanocomposite shows advantages such as low cost and ease of modifications. Like all other inorganic enzyme mimics, it is affected by the change in pH, temperature, concentration of the catalyst and  $\text{H}_2\text{O}_2$ . However, unlike previously reported magnetic nanocomposite for peroxidase mimics, it was synthesized through physical linkage method. This nanocomposite has demonstrated improved peroxidase activity in addition to providing better colloidal stability. In contrast to *in situ* methods already in use, GO-CF nanocomposite was synthesized using simple two steps mini emulsion method. This method was not only quick but also provided better control over reaction chemistry.

In order to create covalent nanocomposite GO was synthesized through improved hummers method whereas bare CoFe nanoparticles synthesized through co-precipitation method were post modified through APTMS polymer to create amine groups at nanoparticles surface. These amine groups of nanoparticles react with carboxyl terminal groups of GO leading to the formation of amide bond between them thereby leading to the formation of covalent GO-CoFe composite. Covalent composites are less likely to be affected by environmental factors such as different pH, temperature and solvent. However in case of covalent nanocomposite formation controlling uniform distribution of the nanoparticles over the GO sheet is a difficult task in addition to this having nanoparticles as free entity in the solution leads to lesser degree of control over the composite.

Few of the future works that can be carried out on these composites for its potential use in biomedical sensing involves the following.

- Further *in vivo* testing of these designed composites is required.
- Elucidating the possibility of potential adverse effect of surface physicochemical properties of the composites. This will help in tailoring and translating the designed system to practical applications.
- Design of graphene oxide based magnetic nanocomposite which leads to visible light driven peroxidase activity is another area of attention.
- Evaluating the effect of increase in subsequent Wt % ratio of graphene oxide and CoFe nanoparticles for a given composite towards peroxidase mimetic activity can be carried out.
- Varying the size of nanoparticles will influence the outcome of peroxidase like activity.

- We expect broader utilization of this engineered nanomaterial towards cancer diagnostics through its conjugation with various recognition elements such as aptamers and peptides.

In brief, use of inorganic magnetic nanocomposite as peroxidase mimetic material is expected to surge in near future as it will provide a platform for on demand diagnostics and sensing.

## References

1. Yang, Y., et al., *Graphene based materials for biomedical applications*. *Materials today*, 2013. **16**(10): p. 365-373.
2. Santos, C.M., et al., *Graphene nanocomposite for biomedical applications: fabrication, antimicrobial and cytotoxic investigations*. *Nanotechnology*, 2012. **23**(39): p. 395101.
3. Orecchioni, M., et al., *Graphene as cancer theranostic tool: progress and future challenges*. *Theranostics*, 2015. **5**(7): p. 710.
4. Zamboni, W.C., et al., *Best practices in cancer nanotechnology: perspective from NCI nanotechnology alliance*. *Clinical cancer research*, 2012. **18**(12): p. 3229-3241.
5. Goenka, S., V. Sant, and S. Sant, *Graphene-based nanomaterials for drug delivery and tissue engineering*. *Journal of Controlled Release*, 2014. **173**: p. 75-88.
6. Das, T.K. and S. Prusty, *Graphene-based polymer composites and their applications*. *Polymer-Plastics Technology and Engineering*, 2013. **52**(4): p. 319-331.
7. Servant, A., et al., *Graphene for multi-functional synthetic biology: The last 'zeitgeist' in nanomedicine*. *Bioorganic & medicinal chemistry letters*, 2014. **24**(7): p. 1638-1649.
8. Li, W., et al., *3D Graphene Oxide–Polymer Hydrogel: Near-Infrared Light-Triggered Active Scaffold for Reversible Cell Capture and On-Demand Release*. *Advanced Materials*, 2013. **25**(46): p. 6737-6743.
9. Singh, S.K., et al., *Amine-modified graphene: thrombo-protective safer alternative to graphene oxide for biomedical applications*. *Acs Nano*, 2012. **6**(3): p. 2731-2740.
10. Ghaderi, A., et al., *Keys and regulators of nanoscale theranostics*.
11. Duch, M.C., et al., *Minimizing oxidation and stable nanoscale dispersion improves the biocompatibility of graphene in the lung*. *Nano letters*, 2011. **11**(12): p. 5201-5207.

12. Yang, K., et al., *Nano-graphene in biomedicine: theranostic applications*. Chemical Society Reviews, 2013. **42**(2): p. 530-547.
13. Liao, K.-H., et al., *Cytotoxicity of graphene oxide and graphene in human erythrocytes and skin fibroblasts*. ACS applied materials & interfaces, 2011. **3**(7): p. 2607-2615.
14. Shi, S., et al., *Surface engineering of graphene-based nanomaterials for biomedical applications*. Bioconjugate chemistry, 2014. **25**(9): p. 1609-1619.
15. Pan, Y., et al., *Water-Soluble Poly (N-isopropylacrylamide)–Graphene Sheets Synthesized via Click Chemistry for Drug Delivery*. Advanced Functional Materials, 2011. **21**(14): p. 2754-2763.
16. Dimiev, A.M. and J.M. Tour, *Mechanism of graphene oxide formation*. ACS nano, 2014. **8**(3): p. 3060-3068.
17. Peng, E., et al., *Synthesis of Manganese Ferrite/Graphene Oxide Nanocomposites for Biomedical Applications*. Small, 2012. **8**(23): p. 3620-3630.
18. Liu, J., L. Cui, and D. Losic, *Graphene and graphene oxide as new nanocarriers for drug delivery applications*. Acta biomaterialia, 2013. **9**(12): p. 9243-9257.
19. Yang, X., et al., *Multi-functionalized graphene oxide based anticancer drug-carrier with dual-targeting function and pH-sensitivity*. Journal of materials chemistry, 2011. **21**(10): p. 3448-3454.
20. Ito, A., et al., *Medical application of functionalized magnetic nanoparticles*. Journal of bioscience and bioengineering, 2005. **100**(1): p. 1-11.
21. Grass, R.N., E.K. Athanassiou, and W.J. Stark, *Covalently functionalized cobalt nanoparticles as a platform for magnetic separations in organic synthesis*. Angewandte Chemie International Edition, 2007. **46**(26): p. 4909-4912.
22. Kiew, S.F., et al., *Assessing biocompatibility of graphene oxide-based nanocarriers: A review*. Journal of Controlled Release, 2016.
23. Steiner, J.M., *Nanoparticle "theranostic" platforms for applications in cancer*. 2011.
24. Joshi, H.M., et al., *Effects of shape and size of cobalt ferrite nanostructures on their MRI contrast and thermal activation*. The Journal of Physical Chemistry C, 2009. **113**(41): p. 17761-17767.

25. Feng, L., L. Wu, and X. Qu, *New horizons for diagnostics and therapeutic applications of graphene and graphene oxide*. *Advanced Materials*, 2013. **25**(2): p. 168-186.
26. Fu, M., Q. Jiao, and Y. Zhao, *In situ fabrication and characterization of cobalt ferrite nanorods/graphene composites*. *Materials Characterization*, 2013. **86**: p. 303-315.
27. Meyer, J.C., et al., *The structure of suspended graphene sheets*. *Nature*, 2007. **446**(7131): p. 60-63.
28. Zhu, Y., et al., *Graphene and graphene oxide: synthesis, properties, and applications*. *Advanced materials*, 2010. **22**(35): p. 3906-3924.
29. Liu, J., J. Tang, and J.J. Gooding, *Strategies for chemical modification of graphene and applications of chemically modified graphene*. *Journal of Materials Chemistry*, 2012. **22**(25): p. 12435-12452.
30. Sasidharan, A., et al., *Differential nano-bio interactions and toxicity effects of pristine versus functionalized graphene*. *Nanoscale*, 2011. **3**(6): p. 2461-2464.
31. Shen, H., et al., *Biomedical applications of graphene*. *Theranostics*, 2012. **2**(3): p. 283.
32. Pan, Y., N.G. Sahoo, and L. Li, *The application of graphene oxide in drug delivery*. *Expert opinion on drug delivery*, 2012. **9**(11): p. 1365-1376.
33. Huang, C.-L., et al., *Application of paramagnetic graphene quantum dots as a platform for simultaneous dual-modality bioimaging and tumor-targeted drug delivery*. *Journal of Materials Chemistry B*, 2015. **3**(4): p. 651-664.
34. Wang, Y., et al., *Aptamer/graphene oxide nanocomplex for in situ molecular probing in living cells*. *Journal of the American Chemical Society*, 2010. **132**(27): p. 9274-9276.
35. Conde, J., *The Golden Age in Cancer Nanobiotechnology: Quo Vadis?* *Frontiers in bioengineering and biotechnology*, 2015. **3**.
36. Dikin, D.A., et al., *Preparation and characterization of graphene oxide paper*. *Nature*, 2007. **448**(7152): p. 457-460.
37. Sambasivudu, K. and M. Yashwant, *Challenges and opportunities for the mass production of high quality graphene: an analysis of worldwide patents*. *Nanotech Insights*, 2012.
38. Marcano, D.C., et al., *Improved synthesis of graphene oxide*. *ACS nano*, 2010. **4**(8): p. 4806-4814.

39. Chen, T., et al. *High throughput exfoliation of graphene oxide from expanded graphite with assistance of strong oxidant in modified Hummers method.* in *Journal of Physics: Conference Series*. 2009. IOP Publishing.
40. Chen, J., et al., *An improved Hummers method for eco-friendly synthesis of graphene oxide.* *Carbon*, 2013. **64**: p. 225-229.
41. Sun, Z., et al., *Growth of graphene from solid carbon sources.* *Nature*, 2010. **468**(7323): p. 549-552.
42. Dreyer, D.R., et al., *The chemistry of graphene oxide.* *Chemical Society Reviews*, 2010. **39**(1): p. 228-240.
43. Wang, K., et al., *Biocompatibility of graphene oxide.* *Nanoscale Res Lett*, 2011. **6**(8): p. 1-8.
44. Kim, Y.-K., M.-H. Kim, and D.-H. Min, *Biocompatible reduced graphene oxide prepared by using dextran as a multifunctional reducing agent.* *Chemical Communications*, 2011. **47**(11): p. 3195-3197.
45. Park, S., et al., *Biocompatible, Robust Free-Standing Paper Composed of a TWEEN/Graphene Composite.* *Advanced Materials*, 2010. **22**(15): p. 1736-1740.
46. You, P., et al., *Graphene Oxide-Based Nanocarriers for Cancer Imaging and Drug Delivery.* *Current pharmaceutical design*, 2015. **21**(22): p. 3215-3222.
47. Xu, Z., et al., *Covalent functionalization of graphene oxide with biocompatible poly (ethylene glycol) for delivery of paclitaxel.* *ACS applied materials & interfaces*, 2014. **6**(19): p. 17268-17276.
48. Chen, W., et al., *Composites of aminodextran-coated Fe<sub>3</sub>O<sub>4</sub> nanoparticles and graphene oxide for cellular magnetic resonance imaging.* *ACS applied materials & interfaces*, 2011. **3**(10): p. 4085-4091.
49. Fullerton, R.J., et al., *Graphene non-covalently tethered with magnetic nanoparticles.* *Carbon*, 2014. **72**: p. 192-199.
50. Kiew, S.F., et al., *Assessing biocompatibility of graphene oxide-based nanocarriers: A review.* *Journal of Controlled Release*, 2016. **226**: p. 217-228.
51. Zhou, L., et al., *Combination of chemotherapy and photodynamic therapy using graphene oxide as drug delivery system.* *Journal of Photochemistry and Photobiology B: Biology*, 2014. **135**: p. 7-16.

52. Hou, C., et al., *Facile synthesis of water-dispersible Cu<sub>2</sub>O nanocrystal-reduced graphene oxide hybrid as a promising cancer therapeutic agent*. *Nanoscale*, 2013. **5**(3): p. 1227-1232.
53. Shi, X., et al., *Graphene-based magnetic plasmonic nanocomposite for dual bioimaging and photothermal therapy*. *Biomaterials*, 2013. **34**(20): p. 4786-4793.
54. Miao, W., et al., *Image-guided synergistic photothermal therapy using photoresponsive imaging agent-loaded graphene-based nanosheets*. *Journal of Controlled Release*, 2015.
55. Tian, B., et al., *Photothermally enhanced photodynamic therapy delivered by nano-graphene oxide*. *ACS nano*, 2011. **5**(9): p. 7000-7009.
56. Abdolahad, M., et al., *Polyphenols attached graphene nanosheets for high efficiency NIR mediated photodestruction of cancer cells*. *Materials Science and Engineering: C*, 2013. **33**(3): p. 1498-1505.
57. Sheng, Z., et al., *Protein-assisted fabrication of nano-reduced graphene oxide for combined in vivo photoacoustic imaging and photothermal therapy*. *Biomaterials*, 2013. **34**(21): p. 5236-5243.
58. Chen, L., et al., *Radionuclide <sup>131</sup>I labeled reduced graphene oxide for nuclear imaging guided combined radio-and photothermal therapy of cancer*. *Biomaterials*, 2015. **66**: p. 21-28.
59. Robinson, J.T., et al., *Ultrasmall reduced graphene oxide with high near-infrared absorbance for photothermal therapy*. *Journal of the American Chemical Society*, 2011. **133**(17): p. 6825-6831.
60. Kumar, S., et al., *Graphene based multifunctional superbots*. *Carbon*, 2015. **89**: p. 31-40.
61. Lima-Tenório, M.K., et al., *Magnetic nanoparticles: In vivo cancer diagnosis and therapy*. *International journal of pharmaceutics*, 2015. **493**(1): p. 313-327.
62. Rao, J.P., P. Gruenberg, and K.E. Geckeler, *Magnetic zero-valent metal polymer nanoparticles: Current trends, scope, and perspectives*. *Progress in Polymer Science*, 2015. **40**: p. 138-147.
63. Ahmed, N., H. Fessi, and A. Elaissari, *Theranostic applications of nanoparticles in cancer*. *Drug discovery today*, 2012. **17**(17): p. 928-934.

64. Sharifi, I., H. Shokrollahi, and S. Amiri, *Ferrite-based magnetic nanofluids used in hyperthermia applications*. Journal of Magnetism and Magnetic Materials, 2012. **324**(6): p. 903-915.
65. Laurent, S., et al., *Magnetic iron oxide nanoparticles: synthesis, stabilization, vectorization, physicochemical characterizations, and biological applications*. Chemical reviews, 2008. **108**(6): p. 2064-2110.
66. Kharisov, B.I., et al., *Solubilization, dispersion and stabilization of magnetic nanoparticles in water and non-aqueous solvents: recent trends*. RSC Advances, 2014. **4**(85): p. 45354-45381.
67. Qiu, X.-L., et al., *One-pot solvothermal synthesis of biocompatible magnetic nanoparticles mediated by cucurbit [n] urils*. Journal of Materials Chemistry C, 2015. **3**(15): p. 3517-3521.
68. Anbarasu, M., et al., *Synthesis and characterization of polyethylene glycol (PEG) coated Fe<sub>3</sub>O<sub>4</sub> nanoparticles by chemical co-precipitation method for biomedical applications*. Spectrochimica Acta Part A: Molecular and Biomolecular Spectroscopy, 2015. **135**: p. 536-539.
69. Freitas, J.C.d., et al., *Magnetic Nanoparticles Obtained by Homogeneous Coprecipitation Sonochemically Assisted*. Materials Research, 2015. **18**: p. 220-224.
70. Zhang, Y., et al., *Magnetic properties for the single-domain CoFe<sub>2</sub>O<sub>4</sub> nanoparticles synthesized by the hydrothermal method*. Journal of Wuhan University of Technology-Mater. Sci. Ed., 2015. **30**(6): p. 1140-1146.
71. Altun, S., et al., *A facile and effective immobilization of glucose oxidase on tannic acid modified CoFe<sub>2</sub>O<sub>4</sub> magnetic nanoparticles*. Colloids and Surfaces B: Biointerfaces, 2015. **136**: p. 963-970.
72. Ciciliati, M.A., et al., *Fe-doped ZnO nanoparticles: Synthesis by a modified sol-gel method and characterization*. Materials Letters, 2015. **159**: p. 84-86.
73. Jovanović, S., et al., *Effect of oleic acid concentration on the physicochemical properties of cobalt ferrite nanoparticles*. The Journal of Physical Chemistry C, 2014. **118**(25): p. 13844-13856.
74. Verma, J., S. Lal, and C.J. Van Noorden, *Nanoparticles for hyperthermic therapy: synthesis strategies and applications in glioblastoma*. 2014.

75. Cotica, L.F., et al. *Thermal decomposition synthesis and assessment of effects on blood cells and in vivo damages of cobalt ferrite nanoparticles*. in *Journal of Nano Research*. 2014. Trans Tech Publ.
76. Wei, Y., et al., *Biocompatible Low-Retention Superparamagnetic Iron Oxide Nanoclusters as Contrast Agents for Magnetic Resonance Imaging of Liver Tumor*. *Journal of biomedical nanotechnology*, 2015. **11**(5): p. 854-864.
77. Lee, N., et al., *Iron Oxide Based Nanoparticles for Multimodal Imaging and Magnetoresponse Therapy*. *Chemical Reviews*, 2015. **115**(19): p. 10637-10689.
78. Fan, X., et al., *Magnetic Fe<sub>3</sub>O<sub>4</sub>-graphene composites as targeted drug nanocarriers for pH-activated release*. *Nanoscale*, 2013. **5**(3): p. 1143-1152.
79. Feng, L., et al., *A graphene functionalized electrochemical aptasensor for selective label-free detection of cancer cells*. *Biomaterials*, 2011. **32**(11): p. 2930-2937.
80. Urbas, K., et al., *Chemical and magnetic functionalization of graphene oxide as a route to enhance its biocompatibility*. *Nanoscale research letters*, 2014. **9**(1): p. 1-12.
81. Vadukumpully, S., et al., *Flexible conductive graphene/poly (vinyl chloride) composite thin films with high mechanical strength and thermal stability*. *Carbon*, 2011. **49**(1): p. 198-205.
82. Nanda, S.S., G.C. Papaefthymiou, and D.K. Yi, *Functionalization of Graphene Oxide and its Biomedical Applications*. *Critical Reviews in Solid State and Materials Sciences*, 2015(40): p. 292-309.
83. Ma, X., et al., *A functionalized graphene oxide-iron oxide nanocomposite for magnetically targeted drug delivery, photothermal therapy, and magnetic resonance imaging*. *Nano Research*, 2012. **5**(3): p. 199-212.
84. Yu, W., et al., *Highly efficient method for preparing homogeneous and stable colloids containing graphene oxide*. *Nanoscale Research Letters*, 2011. **6**(1): p. 1-7.
85. Shang, J., et al., *The origin of fluorescence from graphene oxide*. *Scientific reports*, 2012. **2**.
86. Liu, S., et al., *Antibacterial activity of graphite, graphite oxide, graphene oxide, and reduced graphene oxide: membrane and oxidative stress*. *Acs Nano*, 2011. **5**(9): p. 6971-6980.

87. Jung, J.H., et al., *A Graphene Oxide Based Immuno-biosensor for Pathogen Detection*. *Angewandte Chemie International Edition*, 2010. **49**(33): p. 5708-5711.
88. Wang, H., et al., *Graphene oxide-peptide conjugate as an intracellular protease sensor for caspase-3 activation imaging in live cells*. *Angewandte Chemie International Edition*, 2011. **50**(31): p. 7065-7069.
89. Hajipour, M.J., et al., *Hyperthermia-induced protein corona improves the therapeutic effects of zinc ferrite spinel-graphene sheets against cancer*. *RSC Advances*, 2014. **4**(107): p. 62557-62565.
90. Peng, E., J. Ding, and J.M. Xue, *Concentration-dependent magnetic hyperthermic response of manganese ferrite-loaded ultrasmall graphene oxide nanocomposites*. *New Journal of Chemistry*, 2014. **38**(6): p. 2312-2319.
91. Loh, K.P., et al., *Graphene oxide as a chemically tunable platform for optical applications*. *Nature chemistry*, 2010. **2**(12): p. 1015-1024.
92. Liu, Z., et al., *PEGylated nanographene oxide for delivery of water-insoluble cancer drugs*. *Journal of the American Chemical Society*, 2008. **130**(33): p. 10876-10877.
93. Zhang, L., et al., *Functional graphene oxide as a nanocarrier for controlled loading and targeted delivery of mixed anticancer drugs*. *Small*, 2010. **6**(4): p. 537-544.
94. Kakran, M., et al., *Functionalized graphene oxide as nanocarrier for loading and delivery of ellagic acid*. *Current medicinal chemistry*, 2011. **18**(29): p. 4503-4512.
95. Liu, K., et al., *Green and facile synthesis of highly biocompatible graphene nanosheets and its application for cellular imaging and drug delivery*. *Journal of Materials Chemistry*, 2011. **21**(32): p. 12034-12040.
96. Bao, H., et al., *Chitosan-Functionalized Graphene Oxide as a Nanocarrier for Drug and Gene Delivery*. *Small*, 2011. **7**(11): p. 1569-1578.
97. Ma, X., et al., *Graphene oxide wrapped gold nanoparticles for intracellular Raman imaging and drug delivery*. *Journal of Materials Chemistry B*, 2013. **1**(47): p. 6495-6500.

98. Kurapati, R. and A.M. Raichur, *Near-infrared light-responsive graphene oxide composite multilayer capsules: a novel route for remote controlled drug delivery*. Chemical Communications, 2013. **49**(7): p. 734-736.
99. Misra, S.K., et al., *Graphene as a nanocarrier for tamoxifen induces apoptosis in transformed cancer cell lines of different origins*. Small, 2012. **8**(1): p. 131-143.
100. Ma, D., et al., *In situ gelation and sustained release of an antitumor drug by graphene oxide nanosheets*. Carbon, 2012. **50**(8): p. 3001-3007.
101. Xu, Y., et al., *Three-dimensional self-assembly of graphene oxide and DNA into multifunctional hydrogels*. ACS nano, 2010. **4**(12): p. 7358-7362.
102. Yang, Y., et al., *Construction of a graphene oxide based noncovalent multiple nanosupramolecular assembly as a scaffold for drug delivery*. Chemistry-A European Journal, 2012. **18**(14): p. 4208-4215.
103. Zhang, L., et al., *Enhanced Chemotherapy Efficacy by Sequential Delivery of siRNA and Anticancer Drugs Using PEI-Grafted Graphene Oxide*. Small, 2011. **7**(4): p. 460-464.
104. Wu, J., et al., *Graphene oxide used as a carrier for adriamycin can reverse drug resistance in breast cancer cells*. Nanotechnology, 2012. **23**(35): p. 355101.
105. Stavrovskaya, A., *Cellular mechanisms of multidrug resistance of tumor cells*. BIOCHEMISTRY C/C OF BIOKHIMIJA, 2000. **65**(1): p. 95-106.
106. Yang, X., et al., *The preparation of functionalized graphene oxide for targeted intracellular delivery of siRNA*. Journal of Materials Chemistry, 2012. **22**(14): p. 6649-6654.
107. Yan, L., et al., *The use of polyethylenimine-modified graphene oxide as a nanocarrier for transferring hydrophobic nanocrystals into water to produce water-dispersible hybrids for use in drug delivery*. Carbon, 2013. **57**: p. 120-129.
108. Turcheniuk, K., et al., *Insulin loaded iron magnetic nanoparticle-graphene oxide composites: synthesis, characterization and application for in vivo delivery of insulin*. RSC Advances, 2014. **4**(2): p. 865-875.
109. Zhang, Y., et al., *Controlled assembly of Fe<sub>3</sub>O<sub>4</sub> magnetic nanoparticles on graphene oxide*. Nanoscale, 2011. **3**(4): p. 1446-1450.

110. Chaudhari, N.S., et al., *Graphene oxide based magnetic nanocomposites for efficient treatment of breast cancer*. *Materials Science and Engineering: C*, 2014. **37**: p. 278-285.
111. Wang, H., et al., *Chlorotoxin-conjugated graphene oxide for targeted delivery of an anticancer drug*. *International journal of nanomedicine*, 2014. **9**: p. 1433.
112. Weaver, C.L., et al., *Electrically controlled drug delivery from graphene oxide nanocomposite films*. *ACS nano*, 2014. **8**(2): p. 1834-1843.
113. Wang, Y., et al., *Graphene and graphene oxide: biofunctionalization and applications in biotechnology*. *Trends in biotechnology*, 2011. **29**(5): p. 205-212.
114. Luo, M., et al., *Chemiluminescence biosensors for DNA detection using graphene oxide and a horseradish peroxidase-mimicking DNAzyme*. *Chemical Communications*, 2012. **48**(8): p. 1126-1128.
115. Zhu, S., et al., *Strongly green-photoluminescent graphene quantum dots for bioimaging applications*. *Chem. Commun.*, 2011. **47**(24): p. 6858-6860.
116. Wang, Z., et al., *A nanoscale graphene oxide-peptide biosensor for real-time specific biomarker detection on the cell surface*. *Chemical Communications*, 2012. **48**(78): p. 9768-9770.
117. Liu, M., et al., *Distance-independent quenching of quantum dots by nanoscale-graphene in self-assembled sandwich immunoassay*. *Chemical Communications*, 2010. **46**(42): p. 7909-7911.
118. Pu, Y., et al., *Insulin-binding aptamer-conjugated graphene oxide for insulin detection*. *Analyst*, 2011. **136**(20): p. 4138-4140.
119. Jin, Y., et al., *Graphene oxide modified PLA microcapsules containing gold nanoparticles for ultrasonic/CT bimodal imaging guided photothermal tumor therapy*. *Biomaterials*, 2013. **34**(20): p. 4794-4802.
120. Zhou, Y., et al., *Investigation of the effect of phytohormone on the expression of microRNA-159a in Arabidopsis thaliana seedlings based on mimic enzyme catalysis systematic electrochemical biosensor*. *Biosensors and Bioelectronics*, 2014. **54**: p. 244-250.
121. Zhang, H., et al., *Graphene oxide-BaGdF<sub>5</sub> nanocomposites for multi-modal imaging and photothermal therapy*. *Biomaterials*, 2015. **42**: p. 66-77.

122. Rong, P., et al., *Fluorescence dye loaded nano-graphene for multimodal imaging guided photothermal therapy*. RSC Advances, 2016. **6**(3): p. 1894-1901.
123. Lu, W., et al., *Synthesis of Au nanoparticles decorated graphene oxide nanosheets: Noncovalent functionalization by TWEEN 20 in situ reduction of aqueous chloroaurate ions for hydrazine detection and catalytic reduction of 4-nitrophenol*. Journal of hazardous materials, 2011. **197**: p. 320-326.
124. Xu, C., et al., *Synthesis and photoelectrical properties of  $\beta$ -Cyclodextrin functionalized graphene materials with high bio-recognition capability*. Chemical Physics Letters, 2010. **498**(1): p. 162-167.
125. Longoria, A., R. Tinoco, and R. Vázquez-Duhalt, *Chloroperoxidase-mediated transformation of highly halogenated monoaromatic compounds*. Chemosphere, 2008. **72**(3): p. 485-490.
126. Clarke, J., et al., *Development of a quantitative and sensitive enzyme-linked immunosorbent assay for ochratoxin A using antibodies from the yolk of the laying hen*. Journal of Agricultural and Food Chemistry, 1993. **41**(10): p. 1784-1789.
127. He, W., et al., *Enzyme-like activity of nanomaterials*. Journal of Environmental Science and Health, Part C, 2014. **32**(2): p. 186-211.
128. Wilhelmová, N., Cornish-Bowden, A.: *Fundamentals of Enzyme Kinetics*. Biologia Plantarum, 1996. **38**(3): p. 430-430.
129. Guo, Y., et al., *Hemin– graphene hybrid nanosheets with intrinsic peroxidase-like activity for label-free colorimetric detection of single-nucleotide polymorphism*. ACS nano, 2011. **5**(2): p. 1282-1290.
130. Tao, Y., et al., *Self-assembled, functionalized graphene and DNA as a universal platform for colorimetric assays*. Biomaterials, 2013. **34**(20): p. 4810-4817.
131. Liu, M., et al., *Interface engineering catalytic graphene for smart colorimetric biosensing*. ACS nano, 2012. **6**(4): p. 3142-3151.
132. Dutta, S., et al., *Benzoin derived reduced graphene oxide (rGO) and its nanocomposite: application in dye removal and peroxidase-like activity*. RSC Advances, 2013. **3**(44): p. 21475-21483.
133. Hao, J., et al., *In situ controllable growth of CoFe<sub>2</sub>O<sub>4</sub> ferrite nanocubes on graphene for colorimetric detection of hydrogen peroxide*. Journal of Materials Chemistry A, 2013. **1**(13): p. 4352-4357.

134. Long, Y.J., et al., *Visual observation of the mercury-stimulated peroxidase mimetic activity of gold nanoparticles*. Chemical Communications, 2011. **47**(43): p. 11939-11941.
135. Gao, L., et al., *Intrinsic peroxidase-like activity of ferromagnetic nanoparticles*. Nature nanotechnology, 2007. **2**(9): p. 577-583.
136. Liu, M., et al., *Stimuli-responsive peroxidase mimicking at a smart graphene interface*. Chemical Communications, 2012. **48**(56): p. 7055-7057.
137. Liu, W., et al., *Graphene–palladium nanowires based electrochemical sensor using ZnFe<sub>2</sub>O<sub>4</sub>–graphene quantum dots as an effective peroxidase mimic*. Analytica chimica acta, 2014. **852**: p. 181-188.
138. Lin, X.-Q., et al., *Platinum nanoparticles/graphene-oxide hybrid with excellent peroxidase-like activity and its application for cysteine detection*. Analyst, 2015. **140**(15): p. 5251-5256.
139. Song, Y., et al., *Graphene oxide: intrinsic peroxidase catalytic activity and its application to glucose detection*. Advanced Materials, 2010. **22**(19): p. 2206-2210.
140. Qu, F., T. Li, and M. Yang, *Colorimetric platform for visual detection of cancer biomarker based on intrinsic peroxidase activity of graphene oxide*. Biosensors and Bioelectronics, 2011. **26**(9): p. 3927-3931.
141. Dong, Y.-l., et al., *Graphene oxide–Fe<sub>3</sub>O<sub>4</sub> magnetic nanocomposites with peroxidase-like activity for colorimetric detection of glucose*. Nanoscale, 2012. **4**(13): p. 3969-3976.
142. Wang, W., X. Jiang, and K. Chen, *Iron phosphate microflowers as peroxidase mimic and superoxide dismutase mimic for biocatalysis and biosensing*. Chemical Communications, 2012. **48**(58): p. 7289-7291.
143. Feng, X., et al., *Controlled synthesis of monodisperse CoFe<sub>2</sub>O<sub>4</sub> nanoparticles by the phase transfer method and their catalytic activity on methylene blue discoloration with H<sub>2</sub>O<sub>2</sub>*. Journal of Magnetism and Magnetic Materials, 2013. **343**: p. 126-132.
144. Zhang, K., et al., *A simple route to CoFe<sub>2</sub>O<sub>4</sub> nanoparticles with shape and size control and their tunable peroxidase-like activity*. RSC Advances, 2015. **5**(14): p. 10632-10640.

145. Zhang, Y., et al., *Adsorption of Pb (II) and Hg (II) from aqueous solution using magnetic CoFe<sub>2</sub>O<sub>4</sub>-reduced graphene oxide*. Journal of Molecular Liquids, 2014. **191**: p. 177-182.
146. Peng, Y., et al., *Size-and shape-dependent peroxidase-like catalytic activity of MnFe<sub>2</sub>O<sub>4</sub> Nanoparticles and their applications in highly efficient colorimetric detection of target cancer cells*. Dalton Transactions, 2015. **44**(28): p. 12871-12877.
147. Xing, Z., et al., *Two-dimensional hybrid mesoporous Fe<sub>2</sub>O<sub>3</sub>-graphene nanostructures: a highly active and reusable peroxidase mimetic toward rapid, highly sensitive optical detection of glucose*. Biosensors and Bioelectronics, 2014. **52**: p. 452-457.
148. Hsu, K.-I., et al., *Immobilization of iron hydroxide/oxide on reduced graphene oxide: peroxidase-like activity and selective detection of sulfide ions*. RSC Advances, 2014. **4**(71): p. 37705-37713.
149. Zhang, L.-N., et al., *In situ growth of porous platinum nanoparticles on graphene oxide for colorimetric detection of cancer cells*. Analytical chemistry, 2014. **86**(5): p. 2711-2718.
150. Zheng, X., et al., *In Situ Synthesis of Self-Assembled Three-Dimensional Graphene-Magnetic Palladium Nanohybrids with Dual-Enzyme Activity through One-Pot Strategy and Its Application in Glucose Probe*. ACS applied materials & interfaces, 2015. **7**(6): p. 3480-3491.
151. Zhang, S., et al., *A strongly coupled Au/Fe<sub>3</sub>O<sub>4</sub>/GO hybrid material with enhanced nanozyme activity for highly sensitive colorimetric detection, and rapid and efficient removal of Hg<sup>2+</sup> in aqueous solutions*. Nanoscale, 2015. **7**(18): p. 8495-8502.
152. Xie, J., et al., *Co<sub>3</sub>O<sub>4</sub>-reduced graphene oxide nanocomposite as an effective peroxidase mimetic and its application in visual biosensing of glucose*. Analytica chimica acta, 2013. **796**: p. 92-100.
153. Gyergyek, S., M. Drofenik, and D. Makovec, *Oleic-acid-coated CoFe<sub>2</sub>O<sub>4</sub> nanoparticles synthesized by co-precipitation and hydrothermal synthesis*. Materials Chemistry and Physics, 2012. **133**(1): p. 515-522.
154. Kim, Y., et al., *A composite of a graphene oxide derivative as a novel sensing layer in an organic field-effect transistor*. Journal of Materials Chemistry C, 2014. **2**(23): p. 4539-4544.

155. Bu, W., et al., *Oleic acid/oleylamine cooperative-controlled crystallization mechanism for monodisperse tetragonal bipyramid NaLa (MoO<sub>4</sub>)<sub>2</sub> nanocrystals*. The Journal of Physical Chemistry C, 2009. **113**(28): p. 12176-12185.
156. Chen, J., et al., *Water-enhanced oxidation of graphite to graphene oxide with controlled species of oxygenated groups*. Chemical Science, 2016.
157. Pogacean, F., et al., *Graphene based nanomaterials as chemical sensors for hydrogen peroxide—A comparison study of their intrinsic peroxidase catalytic behavior*. Sensors and Actuators B: Chemical, 2015. **213**: p. 474-483.
158. Zhang, X., et al., *Dual-functional Pt-on-Pd supported on reduced graphene oxide hybrids: Peroxidase-mimic activity and an enhanced electrocatalytic oxidation characteristic*. Talanta, 2015. **134**: p. 132-135.
159. Lin, L., et al., *Intrinsic peroxidase-like catalytic activity of nitrogen-doped graphene quantum dots and their application in the colorimetric detection of H<sub>2</sub>O<sub>2</sub> and glucose*. Analytica chimica acta, 2015. **869**: p. 89-95.
160. Mallakpour, S., A. Abdolmaleki, and S. Borandeh, *Fabrication of amino acid-based graphene-zinc oxide (ZnO) hybrid and its application for poly (ester–amide)/graphene-ZnO nanocomposite synthesis*. Journal of Thermoplastic Composite Materials, 2015: p. 0892705715598365.
161. Liu, P., Z. Yao, and J. Zhou, *Controllable synthesis and enhanced microwave absorption properties of silane-modified Ni<sub>0.4</sub>Zn<sub>0.4</sub>Co<sub>0.2</sub>Fe<sub>2</sub>O<sub>4</sub> nanocomposites covered with reduced graphene oxide*. RSC Advances, 2015. **5**(114): p. 93739-93748.